Artificial pancreas under stable pulsatile MPC: Improving the closed-loop performance

P. Abuin [a,*], P.S. Rivadeneira [b], A. Ferramosca [c], A.H. González [a]

[a] *Institute of Technological Development for the Chemical Industry (INTEC), CONICET-Universidad Nacional del Litoral, Güemes 3450, (3000), Santa Fe, Argentina*
[b] *Universidad Nacional de Colombia, Facultad de Minas, Cra. 80#65-224, Medellín, Colombia*
[c] *CONICET, UTN - Facultad Regional de Reconquista, 27 de Abril 1000 (3560), Reconquista, Argentina*

A B S T R A C T

This work presents a pulsatile Zone Model Predictive Control (pZMPC) for the control of blood glucose concentration (BGC) in patients with Type 1 Diabetes Mellitus (T1DM). The main novelties of the algorithm – in contrast to other existing strategies – are: (i) it controls the patient glycemia by injecting short duration insulin boluses for both, the basal and bolus infusions, in an unified manner, (ii) it performs the predictions and estimations (critical to anticipate both, hypo and hyperglycemia) based on a physiological individualized long-term model, (iii) it employs disturbance observers to compensate plant-model mismatches, (iv) it ensures, under standard assumptions, closed-loop stability, and (v) it can be used – under minor modifications – as an optimal basal–bolus calculator to emulate conventional therapies. Because of the latter characteristic, a significantly better performance is achieved, not only in terms of classical indexes (time in the normoglycemia zone, avoidance of hypoglycemia in the short term, avoidance of hyperglycemia in the long term) but also in terms of its applicability (use of the pump or injections). Such a performance is tested in a cohort of in-silico patients from the FDA-accepted UVA/Padova simulation platform, considering the most challenging scenarios.

© 2020 Elsevier Ltd. All rights reserved.

1. Introduction

Type 1 Diabetes Mellitus (T1DM) is a chronic disease, affecting approximately 42 million people around the world (10%–15% of all diabetes cases) [1]. It is characterized by a destruction of pancreatic β cells due to an auto-immune response (T1DMa, 70%–90% cases) or idiopathic causes (T1DMb) [2] leading to a complete deficiency of endogenous insulin production, thus resulting in higher blood glucose (BG) levels (fasting BG: > 126 mg/dL, postprandial BG (2 hs): ≥ 200 mg/dL) [3].

In order to restore euglycemia levels (fasting BG: 80–130 mg/dL, peak postprandial BG (2 hs): < 180 mg/dL [4] the functional insulin treatment (FIT) was proposed as therapeutic way to administer exogenous insulin injections, imitating healthy secretion patterns. This way, a basal insulin is delivered to keep glycemia flat during fasting periods, while a bolus insulin is delivered to counteract postprandial hyperglycemia or bring high glucose levels back to target. Although these doses can be estimated with FIT support tools (i.e., correction factor (CF), insulin to carbs ratio (CR), duration of insulin action (DIA)) [5] according

to BG readings and carb counting values, T1DM patients still need to estimate and administrate insulin by itself, which inherently entails risks, as hypoglycemic and hyperglycemic episodes (due to over/under estimation of meal intake, unpredicted physiological variabilities, among others) [6].

Facing this situation, the automatic insulin delivery based on glycemia measurement (artificial pancreas, AP) was proposed as a way to implement FIT in a closed-loop manner [7]. Basically, it is a medical equipment composed of a continuous glucose monitoring (CGM) sensor, an insulin pump (CSII) and a control algorithm which, based on CGM readings, adjusts the insulin delivery in order to maintain blood glucose concentration in normoglycemia levels. Relying on user interaction requirements (i.e., meal announcements, meal boluses, hypoglycemia treatments, patient-specified correction boluses), APs are classified as hybrid closed-loop (HCL) systems or fully automated closed-loop (FCL) systems [8], being the former dependent on manual user inputs to compensate meals or exercise, while the latter gives corrections insulin doses autonomously.

Multiple control algorithms have been proposed for current AP systems, including Proportional–Integral–Derivative (PID) [9], Fuzzy-Logic [10] and Model Predictive Control (MPC) [11]. Of these strategies, MPCs has shown to be the most promissory

one, because of its ability to anticipate undesired glucose excursion and to compute the insulin dosage fulfilling variable constraints (positivity and maximum constraints). Furthermore, MPC can include, without further complexities, meal digestion dynamics, insulin absorption delays, glucose–insulin dynamics and physical exercise effect by considering the corresponding mathematical prediction model [12]. Many version of MPCs have been implemented in AP systems. They can be classified as [13]: unconstrained MPC [14], multiple-model adaptive MPC [15], zone MPC [16], set-point-based enhanced MPC (eMPC) [17], adaptive MPC [18,19], bi-hormonal MPC [20] and policy-based stochastic MPC [21,22]. These strategies were tested under in-silico simulators (UVA/Padova [23], Cambridge [24], Medtronic Virtual Patient [25]) and also, under in-vivo clinical trials.

Most of the MPCs assume a continuous and constant infusion delivery $u(t)$[U/min] over the time interval between samples (referred as zero-order hold, ZOH, assumption) in spite of the fact that pulsatile injections have shown to be preferable in many senses. On one hand, pumps administer insulin by means of micro boluses [26,27]; that is, discrete time micro-infusions distributed along the sampling time interval, which are comparable to pulsatile injections. On the other hand, the use of pulses has several physiological benefits (in fact, the healthy pancreas segregates insulin in such a way, every 5–10 min, [28,29]). Studies have shown both, experimentally [6,5,30] and theoretically [31,32], that a better postprandial control is achieved by shot boluses, especially in the case of meals with high glycemic index (HGI). Moreover, a pulsatile insulin delivery suppresses more effectively the hepatic glucose release, as stated in [29,33].

According to the latter discussion, the objective of this article is to control the glycemia only by insulin pulses, employing a physiological individualized long-term minimal model of glucose–insulin evolution [34], and a pulsatile Zone Model Predictive Controller (pZMPC) based on the use of artificial optimization variables. This approach shows a number of benefits (in contrast to standard zone MPCs) and guarantees, under full state information and non-persistent disturbance assumptions, recursive feasibility and stability of the closed-loop [35,36]. Furthermore, given that the model describes T1DM glycemia evolution under fasting and prandial conditions, the controller administers both, the basal and postprandial infusions simultaneously (opposite to what is done in all the cited AP controllers). This way, the controllable/stabilizable set of the (positively constrained) system is drastically enlarged, given that when hypoglycemia is predicted (not just seen, but anticipated by the model), the controller is able to quickly suspend the basal insulin delivery. Moreover, this infusion mode permits a super-bolus scheme of administration [5]; that is, an increment in the meals correction bolus while the basal insulin rate is temporarily suspended. This infusion scheme, indeed, shows a better postprandial glycemic control than the conventional ones, mainly due to an increase in the rate of insulin absorption speed [30].

Regarding the meals, even though MPC-based AP is naturally robust to bad announced meals, studies have revealed that its performance is significantly degraded when the size of meals increases [37]. To deal with this condition, two augmented double-integrator observers are proposed to have an offset-free behavior under both, partially-announced and unannounced meals scenarios, as well as to cope with moderate plant-model uncertainties. This way, the proposed controller avoids the need of additional meal detection/estimation algorithms [38]. The general control loop proposed in this work is depicted in Fig. 1, where it can be seen that no additional blocks, such as safety algorithms, boluses corrections, basal corrections, etc., are utilized.

The outline of the paper is as follows. After the introduction of Section 1, Section 2 presents the details of glucose–insulin long-term model, including compartment description and parameter
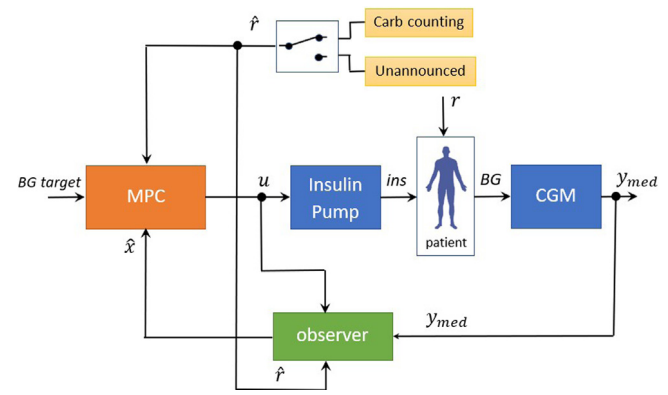
Fig. 1. Control Scheme. The control objective is to maintain the blood glucose (BG) in a safety range (BG target) by manipulating the pulsatile insulin (u) injected to the patient by means of a pump. The blood glucose is measured by a CGM while the meal intake (r) can be (or not) announced by means of meal signal $\hat{r}$ (carb counting associated with meal r or $\hat{r} \equiv 0$ in case of unannounced meal scenario). An observer is used to estimate the current model states $\hat{x}$, based on the CGM signal y_{med}, the insulin infusion rate u and the meal signal $\hat{r}$.

estimation strategy. Later, in Section 3, the relative discretization schemes are formulated in order to get a pulsatile representation of glucose–insulin model, useful for pulse control. In Section 4, the state observer using an augmented double integrator model is formulated; while in Section 5 the pulsatile zone MPC is described including the use of artificial variables and terminal cost to ensure asymptotic stability. Later, in Section 6, an optimal basal–bolus calculator based on an event-triggered formulation is presented. Then, in Section 7 in-silico trials are presented considering announced and unannounced meals scenarios, and a comparison with conventional FIT strategy is done to evaluate the potential advantages of an optimal bolus administration scheme. Finally, in Section 8 some concluding remarks are given.

2. Blood glucose–insulin model

Blood glucose–insulin models can be physiological or data-driven [39,40]. The former are usually based on a compartmental representation [41,24,42], while the latter ones normally rely on time-series approaches [43,44]. Although both kinds of approaches have been used for control-oriented models [45,44,43], physiological-based models are preferable due to their inherent descriptive ability and parameter interpretability. In this work a physiological long-term minimal model based on Ruan proposal [34] is selected as the control-oriented model to be used for both, the state estimator and the pZMPC.

2.1. Glucose dynamics

The glycemia evolution is described by a single compartment:

$$\frac{dG(t)}{dt} = \theta_0 - \theta_1 G(t) - \theta_2 Q_i(t) + \theta_3 Q_g(t) \qquad (1)$$

where $G(t)$ is the blood glucose concentration [mg/dL], $Q_i(t)$ is the insulin delivery rate in plasma [U/min] and $Q_g(t)$ represents the rate of carbohydrate absorption from the gut [g/min]. Furthermore, θ_2 is the insulin sensitivity [mg/(dL · U)] and θ_3 is the carbohydrate factor [mg/(dL · g)], being the rate of glucose appearance in plasma $Ra(t) = \theta_3 Q_g(t)$[mg/(dL · min)]. In contrast to Bergman model [42,46], Eq. (1) considers the insulin action on glucose consumption independent of the glycemia level (as proposed in [47,34]). Moreover, θ_0 is the endogenous glucose production (EGP) at basal levels EGP_b ($\theta_0 = \theta_1 G_b + \theta_2 U_b$, being G_b

and U_b the glucose and insulin basal rates, respectively) [mg/(dL·min)] while θ_1 is the glucose effectiveness [/min] or glucose self-regulation effect to promote its own metabolism (i.e. stimulating glucose uptake by peripheral tissues and suppressing hepatic glucose release) [48].

Remark 1. Note that the FIT tools can be easily derived from Eq. (1). The correction factor (or insulin sensitivity factor) $CF = \theta_2$[mg/(dL·U)], the raise factor (or carbohydrate factor) $RF = \theta_3$[mg/(dL·g)], the carbohydrate-to-insulin ratio (or the number of carbohydrates covered by 1 unit of insulin) $CR = CF/RF = \theta_2/\theta_3$[g/U] and the insulin basal rate $U_b = (\theta_0 - \theta_1 G_b)/\theta_2$[U/min].

2.2. Insulin absorption subsystem

The insulin absorption subsystem represents the insulin pharmacokinetics with the subcutaneous and blood compartments [47,34,49]:

$$\frac{dQ_i(t)}{dt} = -\frac{1}{\theta_4}Q_i(t) + \frac{1}{\theta_4}Q_{i_{sub}}(t),$$
$$\frac{dQ_{i_{sub}}(t)}{dt} = -\frac{1}{\theta_4}Q_{i_{sub}}(t) + \frac{1}{\theta_4}u(t) \tag{2}$$

where $Q_{i_{sub}}(t)$ stands for the insulin delivery rate in the subcutaneous compartment [U/min], θ_4 is the time constant (or time-to-maximum effective insulin concentration) [min] and $u(t)$ is the insulin infusion rate (bolus and basal) [U/min]. Moreover, the insulin on board (IOB) [U] (the amount of insulin remaining in the body from previous insulin boluses), can be expressed as $IOB(t) = \int_0^t (u(\tau) - Q_i(\tau))d\tau$ where $Q_i(\tau)$ is the plasma insulin infusion rate consumed by insulin-dependent tissues and $[0, t]$ the interval where insulin boluses were administrated . Since $u(\tau) - Q_i(\tau) = \theta_4(\dot{Q}_i + \dot{Q}_{i_{sub}})$ (from (2)) and assuming initial conditions equal to zero ($u(0) = 0$, $Q_i(0) = 0$), the IOB becomes $IOB(t) = \theta_4(Q_i(t) + Q_{i_{sub}}(t))$, which is the expression used hereafter for IOB estimation.

2.3. Meals absorption subsystem

The meal absorption subsystem describes the meal-glucose absorption from the stomach to the gut by a two compartmental model [15,47]:

$$\frac{dQ_g(t)}{dt} = -\frac{1}{\theta_5}Q_g(t) + \frac{1}{\theta_5}Q_{sto}(t),$$
$$\frac{dQ_{sto}(t)}{dt} = -\frac{1}{\theta_5}Q_{sto}(t) + \frac{1}{\theta_5}r(t) \tag{3}$$

where Q_{sto} stands for the glucose delivery rate from the stomach [g/min], θ_5 is the time constant (or time-of-maximum appearance rate of glucose in gut $Q_g(t)$)[min] and $r(t)$ is the rate of oral ingested carbohydrates [g/min].

2.4. Affine state space model

According to control purposes, the following affine continuous-time state space model is considered:

$$\dot{x}(t) = Ax(t) + B_u u(t) + B_r r(t) + E, \quad x(0) = x_0,$$
$$y(t) = Cx(t), \tag{4}$$

where $x(t) = [x_1(t) \ x_2(t) \ x_3(t) \ x_4(t) \ x_5(t)]'$, with $x_1 = G$, $x_2 = Q_i$, $x_3 = Q_{i_{sub}}$, $x_4 = Q_g$ and $x_5 = Q_{sto}$. The output $y(t)$ is given by the state component x_1, i.e., the glycemia to be controlled. As before, $u(t)$ is the insulin infusion [U/min] and $r(t)$ is the rate of carbohydrate (CHO) intake [g/min]. E is a constant matrix (affine

term) accounting for the basal steady-state endogenous glucose production (θ_0). The model matrices are given by:

$$A = \begin{pmatrix} -\theta_1 & -\theta_2 & 0 & \theta_3 & 0 \\ 0 & -\frac{1}{\theta_4} & \frac{1}{\theta_4} & 0 & 0 \\ 0 & 0 & -\frac{1}{\theta_4} & 0 & 0 \\ 0 & 0 & 0 & -\frac{1}{\theta_5} & \frac{1}{\theta_5} \\ 0 & 0 & 0 & 0 & -\frac{1}{\theta_5} \end{pmatrix}, \quad B_u = \begin{pmatrix} 0 \\ 0 \\ \frac{1}{\theta_4} \\ 0 \\ 0 \end{pmatrix},$$

$$B_r = \begin{pmatrix} 0 \\ 0 \\ 0 \\ 0 \\ \frac{1}{\theta_5} \end{pmatrix}, \quad E = \begin{pmatrix} \theta_0 \\ 0 \\ 0 \\ 0 \\ 0 \end{pmatrix}, \quad C = \begin{pmatrix} 1 \\ 0 \\ 0 \\ 0 \\ 0 \end{pmatrix}'. \tag{5}$$

Constraints for both, states and inputs are considered, in such a way that $u \in \mathcal{U}$, $x \in \mathcal{X}$, where $\mathcal{U}$ is given by $\mathcal{U} = \{u \in \mathbb{R}_{\geq 0} \mid u \leq U_{max}\}$, with $U_{max} \approx 15$ [U/min]. Given the cyclic variability of parameters (according to circadian cycle) and the risk of hypoglycemia during the night, $\mathcal{X}$ is assumed to take two different values along the day:

$$\mathcal{X} = \mathcal{X}(t)$$
$$\dot{=} \{x \in \mathbb{R}_{\geq 0}^5 \mid G_{hypo} \leq x_1(t) \leq G_{hyper}, \ \theta_4(x_2(t) + x_3(t)) \leq \overline{IOB}(t)\}, \tag{6}$$

where

$$\overline{IOB}(t) \dot{=} \begin{cases} IOB_s + (CHO_{u_b}/CR + \tau \cdot U_b), & t \in [6, \ 22) \ h \\ IOB_s, & t \in [22, \ 6) \ h, \end{cases}$$

$IOB_s = \theta_4 \cdot (x_{2s} + x_{3s}) = \theta_4 \cdot 2U_b$, τ is the temporal allowable interval of basal suspension during post-prandial period (i.e.: under superbolus mode of infusion) [min] and CHO_{ub} is the meal size upper bound in [g] [50]. The bounds for x_1 are given by $G_{hypo} = 60$ and $G_{hyper} = 300$ mg/dL. Note that $\mathcal{X}(t)$ is unbounded for x_4, x_5, which is consistent with the fact that these two state component (associated to the meal ingestion) are uncontrollable.

As part of the system/problem description, a target set $\mathcal{Y}^{Tar}$ representing the normoglycemia is defined as $\mathcal{Y}^{Tar} \dot{=} \{y \in \mathbb{R} : G_{min} \leq y \leq G_{max}\}$, where G_{min} and G_{max} are between 70–80 mg/dL and 140–180 mg/dL, respectively.[1]

2.5. Parameter estimation

Although model (4) is *a-priori* uniquely identifiable, the lack of internal fluxes measurements (i.e. EGP, Ra, IOB) jeopardizes the model plausibility; that is, the physiological feasibility of estimated parameters [51]. Consequently, an identification technique based on regularized least-squares (RLS) by carbohydrate-to-insulin ratio (CR^0), time-to-maximum effective insulin concentration (θ_4^0) and time-to-maximum appearance rate of glucose in gut (or plasma) (θ_5^0) is considered. The proposed objective function is:

$$V_N(\theta) = \frac{\|y(k) - \hat{y}(k)\|^2}{\|y(k) - \overline{y}(k)\|^2} + \theta^0 \alpha \theta^{0'} \tag{7}$$

where $y(k)$ is the measured blood glucose from in-silico patient of UVA/Padova simulator, $\overline{y}(k)$ is its average, $\hat{y}(k)$ is the model predicted output and $\theta^0 = [(\theta_2 - CR^0\theta_3) \ (\theta_4 - \theta_4^0) \ (\theta_5 - \theta_5^0)]$ a regularization term, with $\alpha = diag(1, 1, 1/(\theta_5^0)^2)$. The minimization of (7) is performed using Matlab®*fmincon* routine, with individualized initial parameters given by: $\theta_0(0) = \theta_1(0)G_b +$

---

[1] Note the difference between a constraint set $\mathcal{X}$ and a target set $\mathcal{Y}^{Tar}$, in the sense that the system may be outside the latter during the transient regime, while it must be inside the former at any time. $\mathcal{X}$ is associated to the domain of validity of the model.

$\theta_2(0)U_b$, $\theta_1(0) = \theta_1^0$, $\theta_2(0) = CF$, $\theta_3(0) = RF$, $\theta_4(0) = \theta_4^0$ and $\theta_5(0) = \theta_5^0$, with $\theta_1^0 = 0.004$[min] [34] and $G_b = y(1)$. Note that it is assumed that glycemia is at equilibrium at the beginning of identification.

The parameter CR^0 is established according to CR value of each patient while θ_5^0 is set in 40[min] [15] for all patients (Table 1). Moreover, since an accurate estimation of θ_4 is crucial to avoid insulin stacking problems [49], θ_4^0 is determined by minimizing the sum of squared residuals (least-squares, LS) between the estimated *IOB* and the real value of the simulator (see Remark 2).

The proposed model achieved an acceptable goodness of fit (GoF)[2] : median [25th, 75th] of 48.53 [43.30, 52.90] for 10 individualized in-silico patients (Table 2). Messori et al. [45], using a linearized model of UVA/Padova Model (13 states), reached a GoF of 55.68 [41.22, 66.54] for 100 in-silico adults.

Remark 2. Following the same ideas of Section 2.2, the *IOB* of the UVA/Padova simulator can be computed as $IOB(t) = \int_0^t (u(\tau) - \frac{BW}{6000}R_{ai}(\tau)) d\tau = \frac{BW}{6000}(I_{SC1}(t) + I_{SC2}(t))$, where BW is the body weight [kg], R_{ai} is the rate of appearance of insulin in plasma [pmol/(min·kg)] and, $I_{SC1}(t)$ and $I_{SC2}(t)$ are the insulin in the first and second subcutaneous compartment [pmol/kg], respectively (see [23]).

3. Discrete-time modeling for pulsatile input signals

As discussed before, a better control of BG is achieved by short duration insulin actions [5,31,32]. In this context, pulsatile models – in contrast to zero-order hold assumptions – are necessary to properly describe the patient dynamics.

If the boluses duration is significantly short in comparison with the time period, the impulsive approach (i.e., pulses of infinitesimal duration) is valid [35]. However, in the AP problem, it is not so clear if the (probably fast) insulin injection is quick enough to have a good representation by the impulsive approach. In any case, having a general pulsatile representation (i.e., pulses of arbitrary duration) that accounts for both, the zero-order hold input and impulsive input as particular extreme cases is desired.

Let us consider system (4), a fixed time period (sampling time) $T > 0$ and a pulsatile input signal of the form

$$u(t) = \begin{cases} u(kT), & t \in [kT, kT + \Delta T) \\ 0, & t \in [kT + \Delta T, (k+1)T), \end{cases} \quad (8)$$

for $k \in \mathbb{N}_{\geq 0}$, where $\Delta \in (0, 1]$ is the (arbitrary small) time duration of the pulses. Furthermore consider that the disturbance $r(t)$ is given by $r(t) = r(kT)$, $t \in [kT, (k+1)T)$, $k \in \mathbb{N}_{\geq 0}$, which is the typical zero-order hold assumption.

Now, by sampling the continuous-time solution of system (4) at times $t = kT$, the following discrete-time system is obtained (see Appendix for details):

$$x((k+1)T) = A^d x(kT) + B_u^d u(kT) + B_r^d r(kT) + E^d, \quad (9)$$

where, assuming that $\theta_1 \neq 0$ (in such a way that A is invertible), $A^d \doteq e^{AT}$, $B_u^d \doteq e^{A(T-\Delta T)}A^{-1}(e^{A\Delta T} - I_5)B_u$, $B_r^d \doteq A^{-1}(e^{AT} - I_5)B_r$, $E^d \doteq A^{-1}(e^{AT} - I_5)E$. Matrices A^d, B_r^d and E^d are the discrete-time counterpart of A, B_r and E, respectively, for the fixed time period T, when r and E are piece-wise constant with a period T. On the other side, B_u^d, which depends on ΔT, accounts for the effect of the input u, which is null from ΔT to T.

Remark 3. Discrete-time system (9) accounts for the two extreme cases in which u is a piece-wise constant signal with period T (i.e., the zero-order hold assumption) and in which u is an impulsive input $u(t) = u(kT)\delta(t - kT)$, $t \in [kT, (k+1)T)$, $k \in \mathbb{N}_{\geq 0}$, where $\delta(t)$ is a Dirac delta. In the first case it is $\Delta T = T$ and, so, $B_u^d = A^{-1}(e^{AT} - I_5)B_u$. In the second case it is $\Delta T \to 0$ and, so, $B_u^d = e^{AT}B_u$ (see [35] for details).

The main dynamical characteristic of pulsatile systems (i.e., system (4), controlled by inputs (8), with $\Delta \in (0, 1]$) is that there is a free-response (no control) lapse of time, at each period T. This way, a periodic or pseudo-periodic behavior for the states is observed, even when the sampled system reaches an equilibrium. Next, a characterization of such a concept is made, to proceed, in Section 5, with a rigorous MPC formulation for pulsatile systems.

3.1. Equilibrium characterization under pulsatile inputs

Given that the control objective is to steer the continuous-time system output (glucose) to a desired set, $\mathcal{Y}^{Tar}$, and maintain it there by only applying pulsatile controls, the concept of equilibria for pulsatile systems needs to be defined first. Opposite to the zero-order hold sampling case, the equilibria of the discrete-time system (9) is not a formal equilibrium of the continuous-time system (4). In fact, no formal equilibrium of system (4) can be reached when it is controlled by pulses and, so, a more general equilibrium definition needs to be used.

Consider a bounded and compact set $\mathcal{X}^{Tar} \subseteq \mathcal{X}(t)$, for all $t \geq 0$, such that $C\mathcal{X}^{Tar} = \mathcal{Y}^{Tar}$.

Definition 1 (*Generalized Equilibrium Set* [35]). A set $\mathcal{X}_s^{Tar} \subseteq \mathcal{X}^{Tar}$ is a generalized equilibrium set for (4), with respect to $\mathcal{X}^{Tar}$, if for every $x_s \in \mathcal{X}_s^{Tar}$ it there exists an input $u_s \in \mathcal{U}$ such that (i) states $x(kT)$, $k \in \mathbb{N}_{\geq 0}$, remain at x_s, when u_s is applied (i.e., $u(kT) = u_s$), and (ii) $x(t) \in \mathcal{X}^{Tar}$, for $t \in (kT, (k+1)T]$, $k \in \mathbb{N}$.

Given a set $\mathcal{X}^{Tar}$, two conditions are necessary (under the fasting condition $r(t) \equiv 0$), for a pair (u_s, x_s) to be a generalized equilibrium. The pair (u_s, x_s) must be an equilibrium of the pulsatile discrete-time system (9): $x_s = A^d x_s + B_u^d u_s + E^d$, and the free state evolution starting at x_s, when u_s is applied to the system by pulses, $\varphi(t; x_s, u_s, 0)$, must remains in $\mathcal{X}^{Tar}$ (see Appendix for details): $\varphi(t; x_s, u_s, 0) \in \mathcal{X}^{Tar}$, for $t \in [0, T]$.

The later condition is relevant given that the continuous-time evolution of physiological state variables needs to be controlled at any time (not just at the sampling time), when a stationary condition is reached. Particularly, it ensures that $y(t) \in \mathcal{Y}^{Tar}$, for all t upon convergence.

Given the sets $\mathcal{Y}^{Tar}$ and $\mathcal{X}(t)$ (defined in Section 2.4), it is easy to find an associated state set[3] $\mathcal{X}^{Tar} \subseteq \mathcal{X}(t)$, $t \geq 0$, such that $C\mathcal{X}^{Tar} = \mathcal{Y}^{Tar}$. However, to find a nonempty generalized equilibrium set with respect to it, say $\mathcal{X}_s^{Tar}$, is not trivial. By following similar steps to the ones in [35, Property 3], it is possible to establish mild conditions on system (4) and time period $T > 0$ under which $\mathcal{X}_s^{Tar}$ can be determined. Sets $\mathcal{X}_s^{Tar}$ and $\mathcal{Y}_s^{Tar} = C\mathcal{X}_s^{Tar}$ will be used in Section 5, to formulate a novel pulsatile MPC for AP.

4. State estimation under pulsatile models

Two state observers are proposed in this work to account for plant-model mismatches, considering meals as the more significant disturbance. First, an output disturbance observer (ODO) is

---

[2] The goodness of fit (GoF) is calculated according to $GoF = 100\,(1 - \frac{\|y(k) - \hat{y}(k)\|}{\|y(k) - \bar{y}(k)\|})$.

[3] For instance, $\mathcal{X}^{Tar} = \{x \in \mathbb{R}_{\geq 0}^5 \mid \mathcal{Y}_s^{min} \leq x_1(t) \leq \mathcal{Y}_s^{max}, \ x_2(t) + x_3(t) \leq 2U_b\}$.

Table 1

A-priori parameters for individualization of 10 in-silico adults.

Patient	001	002	003	004	005	006	007	008	009	010
θ_4^0 [min]	56.0	40.0	52.5	59.5	45.5	52.5	47.5	50.0	47.5	50.0
θ_5^0 [min]	40.0	40.0	40.0	40.0	40.0	40.0	40.0	40.0	40.0	40.0
CR [g/U]	19.161	22.484	14.552	19.703	13.469	8.995	18.145	8.793	19.763	13.773
CF [mg/(dL · U)]	43.854	42.101	35.151	53.204	48.019	25.890	42.604	37.062	53.445	39.503

Table 2

Estimated parameters of 10 individualized in-silico adults.

Patient	001	002	003	004	005	006	007	008	009	010
θ_0 [mg/(dL · min)]	1.327	2.011	0.757	1.252	1.036	2.181	1.901	1.057	2.073	1.074
θ_1 [/min]	0.0034	0.0063	0.0010	0.0027	0.00218	0.0081	0.0018	0.0028	0.0058	0.0032
θ_2 [mg/(dL · U)]	44.223	54.185	25.271	58.349	49.843	37.488	79.44	38.425	88.105	34.591
θ_3 [mg/(dL · g)]	2.308	2.410	1.737	2.961	3.871	4.173	4.379	4.370	4.459	2.51
θ_4 [min]	56.001	40.004	52.202	59.502	46.782	52.503	47.505	50.007	50.505	50.503
θ_5 [min]	21.840	14.624	21.516	25.429	28.638	23.511	22.023	26.854	24.461	23.317

formulated under the main assumption that the plant-model mismatch is due to model uncertainty, without considering any external disturbance effect (i.e., unmodeled meal dynamics). Then, an input disturbance observer (IDO) is proposed assuming a plant-model mismatch related to unannounced meals and unmodeled glucose dynamics.

4.1. Output Disturbance Observer (ODO)

In this case, the main assumption is that the measurable state $y(k) = x_1(k)$ is perturbed by a double integrated white noise process $w(k) \sim N(0, \sigma^2)$, which allows for an offset-free estimation when the plant-model mismatch is an impulse, a step or a ramp. Therefore, this disturbance model is proposed in order to cancel unmodeled glycemia effects during fasting (i.e.: constant mismatch) as well as during postprandial (i.e.: ramp mismatch) periods. The augmented model used for the state estimator is given by:

$$
\underbrace{\begin{bmatrix} x(k) \\ d_1(k) \\ d_2(k) \end{bmatrix}}_{} = \underbrace{\begin{bmatrix} A^d & B^o & 0 \\ 0 & 1 & T \\ 0 & 0 & 1 \end{bmatrix}}_{A_{aug}} \underbrace{\begin{bmatrix} x(k-1) \\ d_1(k-1) \\ d_2(k-1) \end{bmatrix}}_{x_{aug}}
$$

$$
+ \underbrace{\begin{bmatrix} B^d \\ 0 \\ 0 \end{bmatrix}}_{B_{aug}} \underbrace{\begin{bmatrix} u(k-1) \\ r(k-1) \\ 1 \end{bmatrix}}_{u_{aug}} + G\,w(k-1)
$$

$$
y(k) = [C \; 0 \; 0]x_{aug} + v(k) \tag{10}
$$

where A^d, $B^d = [B_u^d \; B_r^d \; E^d]$ and C are the pulsatile matrices defined in Section 3 and $B^o = [1\;0\;0\;0\;0]'$. This way, B^o determines how the integrating disturbance $d_1(k)$ [mg/dL] affects the glycemia state $x_1(k)$ (or system output). Moreover, the process noise covariance $Q_{KF} = E[(G\,w(k-1))(G\,w(k-1))'] = G\,E[w(k-1)w(k-1)']\,G'$ and since, $\sigma^2 = E[w(k-1)w(k-1)']$, results in $Q_{KF} = G \cdot \sigma^2 \cdot G'$, being $G = [0 \; k_i \; k_i \; 0 \; 0 \; k_d]'$ the disturbance input distribution matrix. Furthermore, the measurement noise $v(k)$ is assumed as zero-mean white noise $v(k) \sim N(0, R_{KF})$ with covariance $R_{KF} = \sigma_{CGM}^2$.

The augmented state x_{aug} is estimated by the following time-varying Kalman filter (KF) algorithm:

$$
\hat{x}_{aug}(k|k) = A_{aug}\hat{x}_{aug}(k|k-1) + B_{aug}u_{aug} + K(k)(y(k) - C\hat{x}_{aug}(k|k-1)), \tag{11}
$$

where $\hat{x}_{aug} = [\hat{x}, \; \hat{d}_1, \; \hat{d}_2]'$ is the augmented estimated state, and

$$
P(k|k-1) = A_{aug}P(k-1|k-1)A'_{aug} + Q_{KF},
$$

$$
K(k) = P(k|k-1)C'(CP(k|k-1)C' + R_{KF})^{-1},
$$
$$
P(k|k) = (I - K(k)C)P(k|k-1),
$$

are the covariance of the *a-priori* estimation error $x(k) - \hat{x}(k|k-1)$, the KF gain and the covariance of the *a-posteriori* estimation error $x(k) - \hat{x}(k|k)$, respectively. The KF is initialized at $\hat{x}(0) = [G_b \; U_b \; U_b \; 0 \; 0]'$, $\hat{d}_1(0) = 0$, $\hat{d}_2(0) = 0$ and $P(0|0) = P(\infty|\infty)$, where the solution of a discrete algebraic Riccati equation calculates $P(\infty|\infty)$ according to system (11). Since the estimated states are positive physiological variables, a KF with inequality constraints is employed (see: *2.4. Estimate projection with inequality constraints, [52]*).

From Fig. 2, it can be seen, that in spite of the fact that meals are announced with different misestimation errors, the estimated glycemia ($\hat{x}_1$) and insulin on board ($I\hat{O}B$) follow an offset-free behavior in fasting and postprandial periods. In this sense, note that $d_1(k)$ is moved onto a manifold that cancels meal uncertainty effects on glycemia state (i.e.: when meals are unannounced (UA), d_1 increases in such a way that compensates meal uncertainty impact on glycemia state). Note, that this observer is designed to cancel output disturbances, and consequently, Ra is estimated according to the nominal model.
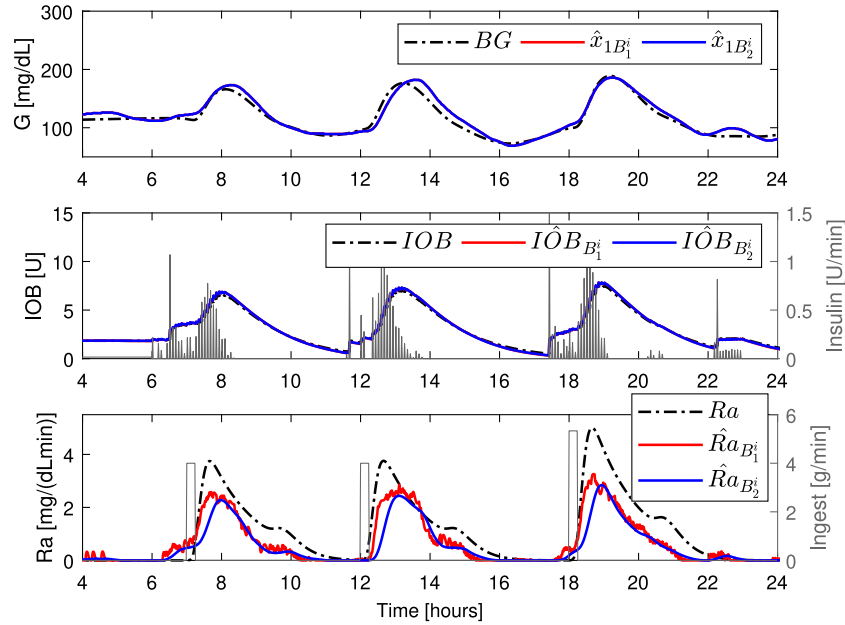
4.2. Input Disturbance Observer (IDO)

Following the same characterization of disturbance dynamics, in this case, it is assumed that uncertainty in the carb counting, denoted by $d_1(k)$ [g/min], is driven by a double integrated white noise process $w(k) \sim N(0, \sigma^2)$. This way, $B_r^d r(k) = B_r^d[\hat{r}(k) + d_1(k)] = B_r^d\hat{r}(k) + B_r^d d_1(k)$, being $r(k)$ the meal ingest rate [g/min] and $\hat{r}(k)$ the carb counting per sampling time [g/min]. We use this disturbance model to ensure offset-free estimation for a large class of meal profiles. In this case, the augmented model is given by (11), but replacing B^o by $B_1^i = B_r^d$ in matrix A_{aug}.

Although this observer explicitly considers the meal dynamic, the augmented double integrator state, $d_1(k)$, implicitly assumes that the plant-model mismatch comes exclusively from this kind of disturbances. Therefore, others source of disturbance, like unmodeled glucose–insulin dynamics, sensor noise, etc., will be explained as a meal ingestion, which may cause an aggressive insulin delivery by the controller. Hence, we proposed to modify B_1^i by $B_2^i = \theta_5 \cdot RF \cdot B^o + \mu \cdot B_r^d$, being θ_5 the meal absorption time constant [min], $RF = \theta_3$ [mg/(dL·g)], $B^o = [0.01 \; 0 \; 0 \; 0 \; 0]'$ and $\mu \in [0, 1]$ a tuning parameter to adjust the aggressiveness (signal-to-noise ratio) of the state observer. Fig. 3 shows that despite the fully input observer with B_1^i is more sensible to unannounced meals (fast rejection), the estimated rate of glucose appearance in plasma ($\hat{Ra}_{B_1^i}$) is affected by uncertainty and noise. On the other hand, the effect of the lumped disturbance d_1 on
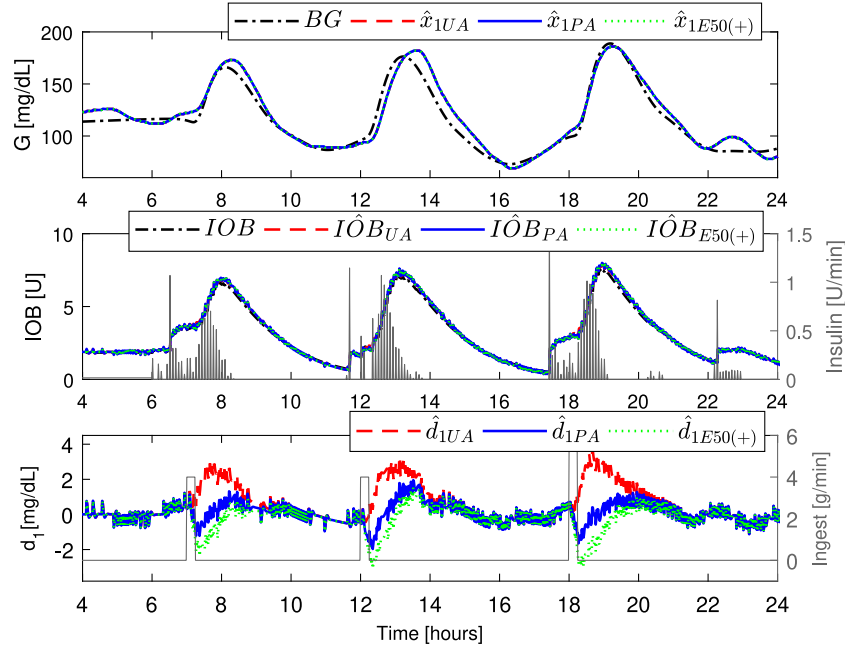
Fig. 2. Performance of the output disturbance observer (ODO) under open-loop, considering unannounced (*UA*), perfectly announced (*PA*) and announcement with +50% estimation error (*E*50(+)) meal ingest. KF setting: $k_i = 1 \cdot 10^{-2}$, $k_d = 1$, $\sigma^2 = 1[mg^2/dL^2]$ and $\sigma^2_{CGM} = 6.51[mg^2/dL^2]$. Patient: Adult 004.

Fig. 3. Performance of the input disturbance observer (IDO) considering $B_1^i = B_r^d$ (red) and $B_2^i = \theta_5 \cdot RF \cdot B^o + \mu \cdot B_r^d$ (blue) under open-loop, unannounced meal case. KF setting: $k_i = 1 \cdot 10^{-2}$, $k_d = 1$, $\sigma^2 = 1[mg^2/dL^2]$, $\sigma^2_{CGM} = 6.51[mg^2/dL^2]$ and $\mu = 0.5$. Patient: Adult 004. (For interpretation of the references to color in this figure legend, the reader is referred to the web version of this article.)

the meal subsystem and glucose dynamic (input observer B_2^i) provides a smoother estimation of *Ra* (see $\hat{Ra}_{B_2^i}$ in Fig. 3). μ is set heuristically at 0.5 for all patients.

5. Pulsatile MPC formulation

In this section, a novel MPC formulation for system (4) is presented, by extending the so-called impulsive zone MPC (iZMPC) presented in [53,35] to the pulsatile case (pZMPC). The glucose

(and state) predictions are based on the discrete-time pulsatile system (9), and the control objective is to drive (and maintain) the blood glucose to a safety zone given by $\mathcal{Y}^{Tar}$, while fulfilling the input and state constraints in the path. The controller is designed for both, the announced (or partially-announced) and the unannounced meal cases. For the former, the meal signal, $\hat{r}$, is the estimated meal ingest rate (or carb counting per sampling time) and the estimated state at the current time, $\hat{x} = \hat{x}(k|k)$, is calculated by the disturbance observer ODO. For the latter, since

no meals are announced ($\hat{r} \equiv 0$), the meal effect is estimated by the disturbance observer IDO, which copes with Ra estimation in cases of unannounced scenarios.

Let consider the sets $\mathcal{Y}_s^{Tar} = C\mathcal{X}_s^{Tar}$, where $\mathcal{X}_s^{Tar}$ is a generalized equilibrium set with respect to $\mathcal{X}^{Tar}$, and both $\mathcal{X}^{Tar} \subseteq \mathcal{X}(t)$, for all $t \geq 0$, and $C\mathcal{X}^{Tar} = \mathcal{Y}^{Tar}$ (as defined in Section 3.1). The cost function of the optimization problem that the MPC solves on-line reads

$$V_N(\hat{x}, \hat{r}, \mathcal{Y}_s^{Tar}; \mathbf{u}, u_a, y_a) \doteq V_{dyn}(\hat{x}, \hat{r}; \mathbf{u}, u_a, y_a) + V_s(\mathcal{Y}_s^{Tar}; u_a, y_a),$$

where

$$V_{dyn}(\hat{x}, \hat{r}; \mathbf{u}, u_a, y_a) \doteq \sum_{j=0}^{N-1} (Cx(j) - y_a)^T Q (Cx(j) - y_a)$$
$$+ (u(j) - u_a)^T R (u(j) - u_a),$$

with $Q > 0$ and $R > 0$, is a term devoted to steer the system to the artificial equilibrium variables $(u_a, y_a) \in \mathcal{U}_s \times \mathcal{Y}_s$, and $V_s(\mathcal{Y}_s^{Tar}; u_a, y_a) \doteq p\left(dist_{\mathcal{Y}_s^{Tar}}(y_a) \right)$, with $p > 0$, and $dist_{\mathcal{A}}(a)$ representing the distance from the point a to the set $\mathcal{A}$, is a stationary cost devoted to steer y_a to the target equilibrium $\mathcal{Y}_s^{Tar}$. As usual in MPC with economic objectives [54,55], the stationary term V_s can be designed to account for objectives that are specific for each application. In Section 5.1, the form of such a cost term is discussed for the case of the AP.

In the latter cost, $\hat{x}$, $\hat{r}$ and $\mathcal{Y}_s^{Tar}$ are optimization parameters, while $\mathbf{u} = \{u(0), u(1), \ldots, u(N-1)\}$, u_a and y_a, are the optimization variables, being N the control horizon. The optimization problem to be solved at the current time k by the MPC is given by $P_{MPC}(\hat{x}, \hat{r}, \mathcal{Y}_s^{Tar})$:

$$\min_{\mathbf{u}, u_a, y_a} V_N(\hat{x}, \hat{r}, \mathcal{Y}_s^{Tar}; \mathbf{u}, u_a, y_a)$$

$$s.t.$$
$$x(0) = \hat{x}, \quad r(0) = \hat{r},$$
$$x(j+1) = A^d x(j) + B_u^d u(j) + B_r^d r(j) + E^d, \quad j \in \mathbb{I}_{0:N-1}$$
$$u(j) \in \mathcal{U}, \quad j \in \mathbb{I}_{0:N-1}$$
$$\tilde{C}x(j) \in \tilde{C}\mathcal{X}(k), \quad j \in \mathbb{I}_{1:N}$$
$$r(j) = 0, \quad j \in \mathbb{I}_{1:N-1}$$
$$\tilde{C}x(N) = x_a,$$
$$y_a = x_{1,a},$$
$$x_a = \tilde{C}A^d x_a + \tilde{C}B^d u_a + \tilde{C}E^d.$$

Given that only the first three states of model (9) are controllable, constraints can be imposed only on the first three states x_1, x_2 and x_3, by means of matrix $\tilde{C} = [I_3 \ 0_{3 \times 2}]$. Furthermore, given that no future meals are considered, r is only used for the first prediction step, if available. Note, that it is assumed that meals are ingested during a sampling period T, although this formulation supports the distribution of the announcement in an arbitrary interval (D_t), in such a way that $D_t = nT$ with $n \in \mathbb{I}_{1:N-1}$. The constraint $\tilde{C}x(N) = x_a$ is the terminal constraint that forces the state at the end of control horizon N to reach the artificial equilibrium state $x_a = [x_{1,a}, x_{2,a}, x_{3,a}]' \in \mathbb{R}^3$. Furthermore, the constraint $x_a = \tilde{C}A^d x_a + \tilde{C}B^d u_a + \tilde{C}E^d$ forces the artificial variable pair (u_a, x_a) to be a feasible equilibrium of the discrete-time system (9) (not necessarily $\mathcal{X}_s$ in the transient regime). The state set $\mathcal{X}(k)$ is a discretization of set $\mathcal{X}(t)$ introduced in (6).

Once the Problem $P_{MPC}(\hat{x}, \hat{r}, \mathcal{Y}_s^{Tar})$ is solved, the (optimal) solution is denoted as $(\mathbf{u}^0, u_a^0, x_a^0)$, while the optimal cost function is given by $V_N^0(\hat{x}, \hat{r}, \mathcal{Y}_s^{Tar}) \doteq V_N(\hat{x}, \hat{r}, \mathcal{Y}_s^{Tar}; \mathbf{u}^0, u_a^0, x_a^0)$. The control law, derived from the application of a **receding horizon control** policy (RHC), is given by $\kappa_{MPC}(\hat{x}, \hat{r}, \mathcal{Y}_s^{Tar}) = u^0(0; x)$, where $u^0(0; x)$ is the first element of the solution sequence $\mathbf{u}^0(x)$.

The main properties of the resulting closed-loop — in the case the state is perfectly measured and no permanent disturbances are considered — are:
(i) The optimization problem $P_{MPC}(x(k), r, \mathcal{Y}_s^{Tar})$, considering $x(k+1) = A^d x(k) + B_u^d \kappa_{MPC}(x(k), 0, \mathcal{Y}_s^{Tar}) + E^d$, is recursively feasible, i.e., if the problem is feasible at $x(\hat{k})$, then it is feasible for all subsequent states $x(k)$, with $k \geq \hat{k}$.
(ii) Set $\mathcal{X}_s^{Tar}$ is stable for the closed loop $x(k+1) = A^d x(k) + B_u^d \kappa_{MPC}(x(k), 0, \mathcal{Y}_s^{Tar}) + E^d$, with a domain of attraction given by the controllable set, in N steps, to the **entire equilibrium set** of system (9), $\mathcal{X}_N$. This means that $y(k) \to \mathcal{Y}_s^{Tar}$ for $k \to \infty$.
(iii) Assuming $x(k)$ reaches $\mathcal{X}_s^{Tar}$ at time $\hat{k}$ ($y(k)$ reaches $\mathcal{Y}_s^{Tar}$), then $x(t)$ will remains in $\mathcal{X}^{Tar}$ for all continuous-time $t \geq \hat{k}T$ ($y(t)$ will remains in $\mathcal{Y}^{Tar}$). This property follows from Definition 1, which accounts for the continuous-time system behavior at the equilibrium set.

The proofs of the latter statements follow similar steps than the one in [35, Theorem 3], and are omitted for the sake of brevity.

5.1. The term V_s

The stationary cost V_s is designed to account for the fact that, mainly in the short term, hypoglycemia is more dangerous than hyperglycemia. That is, V_s is defined by $V_s(\mathcal{Y}_s^{Tar}; u_a, y_a) \doteq \hat{p}\delta_{hyper}^2 + \check{p}\delta_{hypo}^2$, while the following constraint is added to P_{MPC} problem: $\mathcal{Y}_s^{min} - \delta_{hypo} \leq y_a \leq \mathcal{Y}_s^{max} + \delta_{hyper}$. Variables δ_{hypo} and δ_{hyper} are additional optimization variables, constrained to be positive (i.e., $\delta_{hypo} \geq 0$, $\delta_{hyper} \geq 0$), $\hat{p}$ and $\check{p}$ are the weights corresponding to hyper and hypoglycemia, respectively, and $\mathcal{Y}_s^{min}$ and $\mathcal{Y}_s^{max}$ are the limits values of $\mathcal{Y}_s^{Tar}$ (as defined in Section 2.4). This way, by selecting $\hat{p} \ll \check{p}$ an asymmetric cost function, which penalizes harder the hypoglycemic episodes, is obtained. In contrast to other MPC formulations for AP, this asymmetry operates exclusively on the stationary predicted regime, since the artificial variables (u_a, y_a) are generalized equilibrium pairs of the (controllable part of) system (4).

6. Optimal basal–bolus calculator

To further exploit the advantages of pulsatile infusion mode (specifically, postprandial optimal boluses when meals are announced), an optimal basal–bolus calculator based on an event-triggered pZMPC is presented. Basically, the idea is to emulate the conventional FIT, but in an optimal way, in such a way that the controller is switched-on every time a meal is announced, and remains inactive otherwise (no RHC is implemented).

In this case, the cost function of the optimization problem, reads:

$$V_N(\hat{x}, \hat{r}; \mathbf{u}, u_s, \boldsymbol{\delta_{hyper}}, \boldsymbol{\delta_{hypo}})$$
$$= \sum_{j=0}^{N-1} \left(\delta_{hyper}(j)^T \hat{Q} \delta_{hyper}(j) + \delta_{hypo}(j)^T \check{Q} \delta_{hypo}(j) \right.$$
$$\left. + (u(j) - u_s)^T R (u(j) - u_s) \right) + \delta_{hyper}(N)^T \hat{Q} \delta_{hyper}(N)$$
$$+ \delta_{hypo}(N)^T \check{Q} \delta_{hypo}(N)$$

with $\hat{Q} > 0$, $\check{Q} > 0$ and $R > 0$, is an asymmetric cost designed to steer the system directly to $\mathcal{Y}_s^{Tar}$ (without artificial variables), and (u_s, x_s) are just auxiliary equilibrium variable in $\mathcal{U}_s \times \mathcal{X}_s^{Tar}$ being, as before, $\mathcal{X}_s^{Tar}$ a generalized equilibrium set of (4), with $C\mathcal{X}_s^{Tar} = \mathcal{Y}_s^{Tar}$. The optimization problem to be solved by the event-triggered pZMPC, whenever a meal event is announced, reads:

$P_{MPC}(\hat{x}, \hat{r}, \mathcal{Y}_s^{Tar})$:

$$\min_{\mathbf{u}, u_s, \delta_{hyper}, \delta_{hypo}} V_N(\hat{x}, \hat{r}, \mathcal{Y}_s^{Tar}; \mathbf{u}, u_s, \delta_{hyper}, \delta_{hypo})$$

$$s.t.$$

$$
\begin{aligned}
& x(0) = \hat{x}, \quad r(0) = \hat{r}, \\
& x(j+1) = A^d x(j) + B_u^d u(j) \\
& \qquad\qquad + B_r^d r(j) + E^d, && j \in \mathbb{I}_{0:N-1} \\
& u(j) \in \mathcal{U}(k), && j \in \mathbb{I}_{0:N-1} \\
& \tilde{C}x(j) \in \tilde{C}\mathcal{X}(k), && j \in \mathbb{I}_{1:N} \\
& r(j) = 0, && j \in \mathbb{I}_{1:N-1} \\
& \tilde{C}x(N) = x_s, \\
& x_s = \tilde{C}A^d x_s + \tilde{C}B^d u_s + \tilde{C}E^d, \\
& y_s = x_{1,s} \in \mathcal{Y}_s^{Tar} \\
& \mathcal{Y}_s^{min} - \delta_{hypo}(j) \\
& \quad \le Cx(j) \le \mathcal{Y}_s^{max} + \delta_{hyper}(j), && j \in \mathbb{I}_{0:N-1} \\
& \delta_{hypo}(j) \ge 0, \quad \delta_{hyper}(j) \ge 0.
\end{aligned}
$$

The constraints of the problem are basically the same of the original pZMPC of Section 5. The main difference is that no artificial variable are used (u_s and x_s are just auxiliary equilibrium variables, necessary to implement the distance function from the predicted state to the target set $\mathcal{X}_s^{Tar}$) and input constraints are given by $\mathcal{U} = \{u \in \mathbb{R}_{\ge 0} \mid u(0) \le U_{max}, 0 \le u(1) \le 2U_b, u(j) = u(j-1), \text{ for } j \le 2\}$. Under this scheme, the receding horizon policy (RHC) is not used, and the N control actions $\mathbf{u} = \{u(0), u(1), \ldots, u(N-1)\}$ are applied to the system whenever the pZMPC is triggered by a meal event. In summary, the main distinctive characteristics are: (i) the use of an infusion mode constraint to ensure a bolus and basal pattern along the control horizon, (ii) the use of an asymmetric transient stage cost and (iii) each time the controller is activated (meal event), the whole optimal input sequence is implemented. Furthermore, given that in this formulation the domain of attraction, $\mathcal{X}_N$, is reduced (controllable set, in N steps, to target equilibrium set of system (9)), the control horizon N must be enlarged.

7. Simulation results

The benefits of the proposed pulsatile Zone Model Predictive Control (pZMPC) will be demonstrated by means of the commercially available UVA/Padova Type 1 Diabetes Metabolic Simulator (T1DMS2013, Academic Version) with a virtual population of 10 adult patients. Three main cases are simulated, to show how the controller behaves in realistic stressing scenarios. Firstly, an *hybrid closed-loop scheme* is presented, where the meals are announced, perfectly and affected by random misestimation errors. Secondly, the meals become completely unannounced, in a *fully closed-loop scheme*. Thirdly, an *event-triggered scheme* is proposed, where the pZMPC is activated each time a meal is announced, to emulate the conventional FIT set be simulator.

7.1. Description of the scenarios, outcome metrics and statistical analysis

For all the cases, three nominal meals per day are considered: breakfast (60 g CHO, at 7:00), lunch (60 g CHO, at 12:00) and dinner (80 g CHO, at 18:00), affected by random variations in mealtimes (± 10 min) and meal size ($\pm 20\%$) (according to an uniform distribution). The simulation lasts 14 days, and a sampling time of $T = 5$[min], with a pulse size of $\Delta T = 1$[min] are considered. At the beginning (first 6 hs) the virtual patient glycemia is controlled by means of the FIT provided by the UVA/Padova simulator. After that, the insulin treatment (including both, basal rate and boluses) is exclusively managed by the proposed pZMPC. The observers are selected depending on the case: an ODO, for the announced-meal and event-triggered scenarios, and an IDO,

for the unannounced instance. The model noise is the one corresponding to Dexcom G5 Mobile CGM, proposed by Vettoretti et al. [56] (warm-up period omitted), with $a_0 = 1.04$, $b_0 = -1.42$[mg/dL], $c_1 = 1.17$, $\sigma_{CGM}^2 = 6.51$[mg^2/dL^2] and $a_1 = 0$ (no-trend noise). The insulin pump is the default one, provided by the simulator.

In order to assess the performance of the pZMPC, standard metrics (according to the International Consensus on Use of Continuous Glucose Monitoring [57]) are considered. The indexes are given by: mean glucose ($\bar{G}_m$); glucose standard deviation (SD); coefficient of variation (CV); time in range 70–180 mg/dL; time in tight range 70–140 mg/dL; time above 180 and 250 mg/dL, ($G_m > 180$, $G_m > 250$); time below 70 and 54 mg/dL, ($G_m < 70$, $G_m < 54$); number of hypoglycemia events L1 ($G_m < 70$ mg/dL) and L2 ($G_m < 54$ mg/dL); Total Daily Insulin (TDI); and Glucose Management Indicator (GMI) [58], which gives an estimation of laboratory glycosylated hemoglobin (A1c). Postprandial periods (PP) are defined as a 4 hours interval from meal ingest, while night periods (NP) are established from 0:00–6:00 h. All metrics are expressed as median [$25th$, $75th$], with the statistical significance assessed by Wilcoxon signed-rank test. The mean ($\pm$ SD) is reported for hypoglycemia range, with statistical significance according to paired t-test.

### 7.2. Hybrid closed-loop scheme: meal announced case

In this first case, the following scenarios are proposed: perfectly announced meal ingest (*PA*), announcement with carb counting estimation error following the regression curve (Fig.3, [59]) with uniform variability of 30% ($A_{30\%}$) and, announcement with $\pm 50\%$ estimation error ($A_{50\%}$), which is extreme misestimation condition. The ODO presented in Section 4.1 is used as state observer and the meals are directly informed, by considering $\hat{r} = \hat{CHO}/T$, being $\hat{CHO}$ the estimated carbohydrates of meal intake [g], and T the sampling time [min]. Moreover, for all in-silico adults, the controller is tuned by setting $\hat{p} = 1 \cdot 10^9$, $\check{p} = 1 \cdot 10^7$, $Q = 1$ and $R \in [1, 100]$, with the main objective of minimizing the number of hypoglycemic events (*No. L1$_{hypo}$* and *No. L2$_{hypo}$*) as well as maximizing the time on tight target range ($70 \le G_m \le 140$ mg/dL). The control horizon is set on 6 h ($N = 72$) following the American Diabetes Association (ADA) [4] recommendations.

Fig. 4 shows the behavior of the controller when meals are perfectly announced. Insulin is administered in a pulsatile way, fulfilling the glycemia and insulin pharmacokinetics constraints. Moreover, since meals are assumed to be ingested during just one sampling period ($r(0) = \hat{CHO}/T$; $r(j) = 0$, $j > 0$) and the meal absorption subsystem assumes a complete carbohydrate meal profile, the controller compensates the disturbance by a feedback (optimal) super-bolus, which is an expected infusion delivery for this case. Moreover, during fasting periods (i.e.: night period 24:00–30:00 hs, Fig. 4) the pZMPC administrates a pulsatile basal infusion ($u_s \simeq 0.1$[U/min]) which steers the glycemia to the output equilibrium set (according to the equilibrium characterization presented in Section 3.1).

On the other hand, Fig. 5 shows the performance of the controller when meals are announced with a rounding error of $\pm 50\%$ ($A_{50\%}$). In this case, when meals are overestimated (i.e.: $\hat{CHO} = 90$[g]($+50\%$)) the constraint on $\overline{IOB}_{[6,22]}$ becomes active ($\overline{IOB}_{[6,22]} = IOB_s + (CHO_{ub}/CR + \tau \cdot U_b) \simeq 9.10$[U] with $IOB_s = 2.10$[U], $CHO_{ub} = 90$[g], $CR = 22.484$[g/U], $\tau = 120$[min] and $U_b = 0.0255$[U/min]) limiting the insulin infusion. As a result, the hypoglycemic risk related to insulin overdosing due to meal overestimation is reduced.

The performance metrics corresponding to the 14-day scenario are reported in Table 3. As it is expected, the glucose
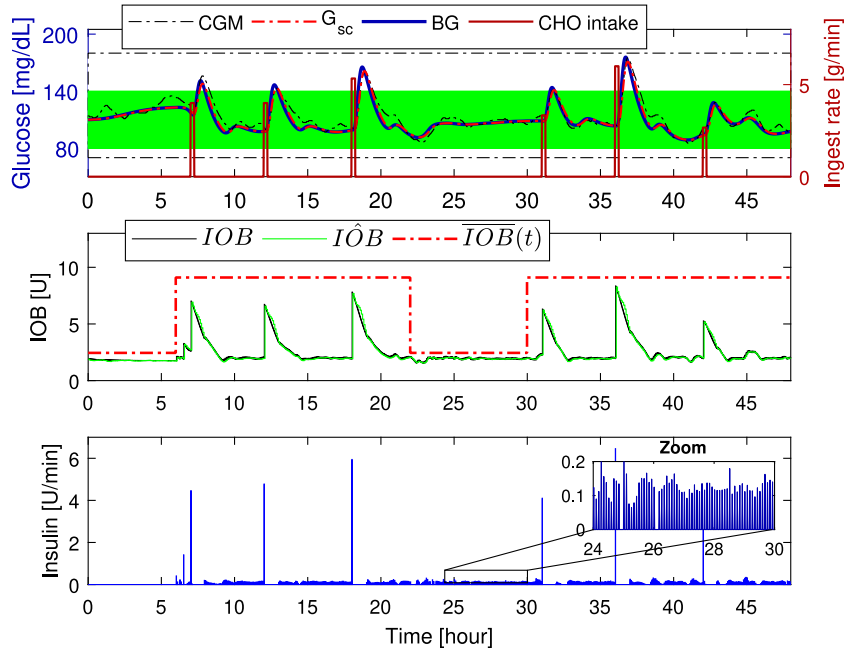
Fig. 4. pZMPC under perfectly announced (PA) case. Above: *CGM*, subcutaneous glucose concentration (G_{sc}), blood glucose (*BG*) and meal ingest rate (*r*). Middle: insulin on board measurement *IOB* and estimation *IÔB*, with $\overline{IOB}(t) = 9.10[U]$ for $t \in [6, \ 22]$ h and $\overline{IOB}(t) = 2.10[U]$ for $t \in [22, \ 6]$ h. Below: insulin pulses *u*[U/min]. Patient: Adult 002. (For interpretation of the references to color in this figure legend, the reader is referred to the web version of this article.)
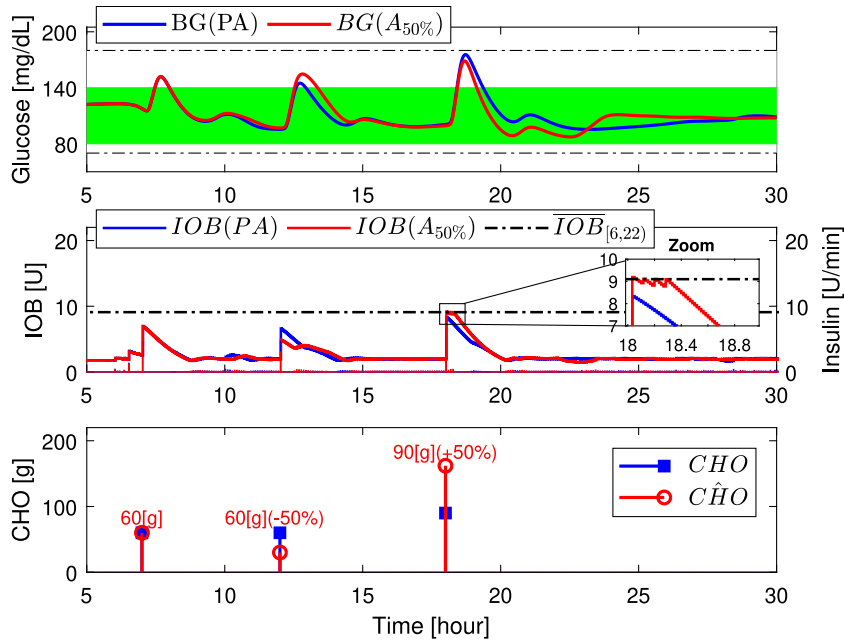
Fig. 5. pZMPC when meals are informed with ±50% error. Above: Blood glucose concentration for PA (blue) and $A_{50\%}$ (red). Middle: IOB measurement for PA (blue) and $A_{50\%}$ (red), and diurnal IOB limit ($\overline{IOB}_{[6,22]}$). Below: carb counting for PA case (blue) and $A_{50\%}$ (red). The sign of percentage indicate the overestimated (+)/ underestimated (−) error. Patient: Adult 002.

variability increases as the carb misestimation becomes higher, being statistical significant for the $A_{50\%}$ case ($SD = 26.047, p < 0.05$). From Fig. 6, which shows the performance of the three scenarios, for the 10 adults, it can be seen that the glycemia variability ([25th, 75th] percentiles) of $A_{50\%}$ is higher than the one of the $A_{30\%}$ and *PA* cases, specially during postprandial periods. Nevertheless, its coefficient of variation ($CV = 21.283, p < 0.05$) is below the upper limit of ($CV < 36\%$) [57], which is in accordance with an stable glucose profile. The time in target range ($70 \leq G_m \leq 180$) is acceptable for the 3 cases, being non-statistically different for $A_{30\%}$, and with a reduction of 1.289% for

$A_{50\%}$ (mainly related with the increment of 1.495% reported in the $G_m > 180$ interval). No hypoglycemia events are reported for *PA* and $A_{30\%}$; while, for $A_{50\%}$ 0.104(0.235) L1 events are registered, due to patient 007. This can be explained, since this patient has an insulin sensitivity index ($S_I \doteq -dG_b/dU_b = \theta_2/\theta_1$) of $4.413 \cdot 10^4[(mg/dL)/(U/min)]$ which is 2.5 times above the cohort mean value of $1.798 \cdot 10^4 (1.266 \cdot 10^4)[(mg/dL)/(U/min)]$.

For the 3 cases, the total daily insulin (TDI) is in order of 43[U/day] which is an expected value being $TDI = BW \cdot 0.53 = 70[kg] \cdot 0.53 \simeq 37[U/day]$. The mean glucose of misestimation cases does not show a significative differences regarding the *PA*

case. The glucose management indicator (GMI) is in order of 6% for the 3 cases, and taking into account that non-significant L1 events happened, it can be concluded that the proposed hybrid closed-loop scheme ensures an appropriated A1c management despite of the carb counting errors.

7.3. Fully closed-loop scheme: meal unannounced case

In this second case, we assess the performance of pZMPC when meals are not announced. The selected observer is the IDO, presented in Section 4.2, which allows for the estimation of meal absorption states $(\hat{x}_4, \hat{x}_5)$, both related to the rate of glucose appearance in plasma $(\hat{Ra})$, when meals are unannounced. For all in-silico patients, the pZMPC is tuned by setting $\hat{p} = 1 \cdot 10^9$, $\check{p} = 1 \cdot 10^3$, $Q = 1 \cdot 10^3$ and $R \in [1, 100]$, tailored following the same objectives of the previous scheme. Penalty $\check{p}$ is reduced in order to increase the relative penalization of hypoglycemia, given that this scheme is more sensible to erratic glucose excursions (especially, related with Ra misestimation). Moreover, matrix Q is increased in order to diminish the glycemia excursion with respect to the euglycemia zone. This tuning parameter is critical, given that meals are sensed by means of the Ra estimation signal $(\hat{Ra})$, which has an inherently delay of $\simeq 50$ min, due to glucose absorption dynamics from the gut ($\simeq 40$ min) plus the glucose measurement delay from the subcutaneous space ($\simeq 10$ min). On the other hand, the IDO is tailored by setting $\mu = 0.5$, for all patients, to smooth down the Ra estimation.

To properly assess the potential improvement in glycemia control achieved by the described scheme (pZMPC + IDO) when meals are not announced (UA_{FCL}), we also simulated the hybrid closed-loop scheme (pZMPC + ODO), but considering a missed announcement scenario (UA_{HCL}). That is, the control scheme of the previous subsection is simulated when some of the meal announcements are lost. Furthermore, the UA_{FCL} is compared with the $A_{30\%}$ case (which is the most realistic case presented in Section 7.2) to assess the significance of glycemia control degradation when meal announcement signal is eliminated from the loop.

Fig. 7 shows that the performance of UA_{FCL} is considerably better than the one of UA_{HCL}: both, median and variability ([25th, 75th] percentiles) are smaller, which is an expected result given that for the former the meal intake is considered as an input disturbance, allowing the controller to provide a faster rejection when $\hat{Ra}$ is increasing. This effect can be seen in the insulin administration pattern, where for the UA_{FCL} case the insulin delivery is higher during postprandial periods, allowing this way a better compensation of the glycemia excursion. Furthermore, from IOB estimation (Fig. 7) it can be seen that, in spite of the fact the UA_{FCL} has a delay of $\simeq 50$ min with respect to the announced case ($A_{30\%}$), the IOB amplitude is in the same order of magnitude for both cases. This explains the fact that glycemia control is not seriously degraded when meals are unannounced.

The performance metrics on the 14-day scenario are presented in Table 4. The UA_{FCL} improves the postprandial control respect to UA_{HCL}, reducing the time above 180 mg/dL to 3.757%($p = 0.0046$), without a significant increment of hypoglycemia events. The results show that the increment of time below $G_m < 70$ mg/dL is non-statistically significant (UA_{FCL} : 0.024(0.056) vs UA_{HCL} : 0.0188(0.0596), $p = 0.85$), although the IDO is naturally more sensible to other disturbances (noise sensor, non modeled plant parts, etc.) than ODO. The glucose variability (SD) is decreased by a 30.466% (UA_{FCL} : 27.839 mg/dL vs UA_{HCL} : 40.037 mg/dL, $p < 0.05$), with an acceptable coefficient of variation ($CV < 36\%$) for the UA_{FCL} case. In addition, the mean glucose is reduced by a 11.5% (UA_{FCL} : 115.95 mg/dL vs UA_{HCL} : 129.22 mg/dL, $p = 0.0028$) which is in accordance with GMI

improvement (UA_{FCL} : 6.084% vs UA_{HCL} : 6.401%, $p = 0.0028$). On the other hand, from comparison between UA_{FCL} and $A_{30\%}$ cases, we can argue that the glycemia control is not considerably degraded when meal announcement signal is removed from the loop. The time within target range ($70 \leq G_m \leq 180$) is only reduced by a 3.0% (UA_{FCL} : 96.243 vs $A_{30\%}$: 99.626, $p < 0.05$), being this fact mainly related to the increment of the time above 180 mg/dL for the UA_{FCL} scheme. No significant hypoglycemia increments are reported. Despite the glucose variability (SD) is higher for the UA_{FCL} case (UA_{FCL} : 27.839 mg/dL vs $A_{30\%}$: 21.014 mg/dL, $p < 0.01$), no significant differences are reported in the mean glycemia management. This is an expected result given that postprandial control is achieved by a sequence of pulses compensating $\hat{Ra}$ increments (in spite of the super-bolus mode of administration). These results suggest that the proposed scheme could replace the hybrid closed-loop under misestimation errors, avoiding the carbohydrate counting.

7.4. Circadian variability

The $A_{30\%}$ and U_{FCL} cases are assessed considering circadian variability of insulin sensitivity. The sensitivity is affected by sinusoidal variations with 24 hours period, random amplitude according to a uniform distribution of $\pm 30\%$ and random phase [60]. Under this scenario, non significative changes are observed respect to the nominal case. For $A_{30\%}$ case, the percentage of time in tight range is 85.186[83.831, 88.163]($p = 0.791$); in 70–180 mg/dL range, 99.546[97.566, 99.679]($p = 0.52$) and above 180 mg/dL, 0.454[0.322, 2.434]($p = 0.499$). Neither L1 and L2 events are reported. On the other hand, for U_{FCL} case, the percentage of time in tight range is 79.223[76.034, 81.100]($p = 0.212$); in 70–180 mg/dL range, 94.585[90.473, 96.976]($p = 0.385$); and above 180 mg/dL, 5.415 [3.0237, 9.527] ($p = 0.385$). The percentage of time in hypoglycemia range (Gm < 70) is 0.0352 (0.0781) ($p = 0.66$) with 0.0143(0.03) ($p = 0.343$) L1 events. As for the nominal case, no L2 event is reported and the percentage of time in hypoglycemia range (Gm < 54) is 0(0). This brief simulation suggest that the inherent robustness of the controller is able to account for this kind of variability. Future research should include the use of time-varying models (floquet) to better account for any circadian variability.

7.5. Event-triggered scheme: meal announced case

In this third case, the performance of the event-triggered pZMPC presented in Section 6 is evaluated. As for the hybrid closed-loop scheme, the output disturbance observer (ODO) is employed, restricting the simulations to perfectly announced case (PA). The control horizon was set in 14 h ($N = 168$) for all patients, except for patient 003, for which it was increased to 24 h ($N = 288$). Notice that this patient has a glucose effectiveness (θ_1) of 0.0010[min] which is 3.8 times below the cohort mean value of 0.0037[/min] (see Table 2).

Fig. 8 shows that the proposed controller (denoted as FIT_{ET}) achieves a better postprandial performance than the conventional therapy, set by the UVA/Padova simulator (denoted as FIT_{CT}). In spite of the fact that both strategies have the same glucose target, the former is tuned to achieve a minimal postprandial hyperglycemia, which is in accordance with glycemia lower bound constraint activation (see [31]), while the latter is adjusted according to more conservative specifications (see: *Determination of CR and CF*, [23]). It is important to note, that the proposed strategy takes into account IOB constraints, avoiding insulin overdosing when meals are misestimated or remaining boluses still active. Furthermore, the pulsatile basal insulin delivery is updated whenever the pZMPC is triggered by a meal
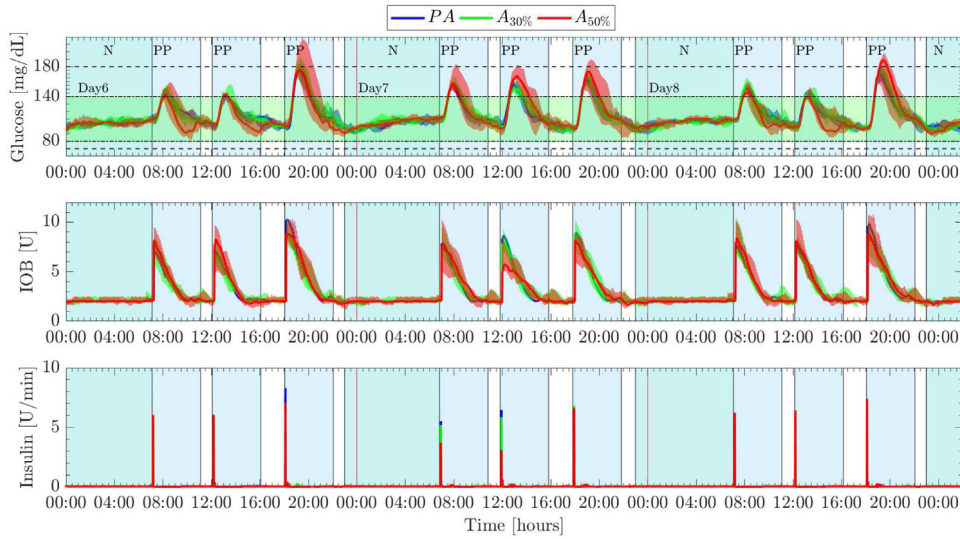
Fig. 6. Hybrid closed-loop controller performance for PA, $A_{30\%}$ and $A_{50\%}$ cases. Glucose, IOB and insulin profiles are shown in terms of median (solid lines) surrounded by colored regions representing the [25th, 75th] percentiles.

Table 3
Performance metrics for hybrid closed-loop scheme under perfectly announced (PA), announcement with randomly 30% misestimation error ($A_{30\%}$) and announcement with $\pm50\%$ error ($A_{50\%}$). An asterisk indicates statistical significance ($p < 0.05$) respect to PA case. (Overall).

|	PA	$A_{30\%}$	$A_{50\%}$
Mean G_m [mg/dL]	114.013 [112.197, 117.590]	114.673 [112.430, 118.417]	114.025 [110.467, 117.317]
SD [mg/dL]	18.648 [16.217, 22.034]	21.014 [16.828, 23.827]	26.047 [18.481, 27.487]*
CV [%]	16.464 [14.573, 19.639]	18.325 [15.030, 19.924]	21.283 [16.736, 23.430]*
$70 \leq G_m \leq 140$ [%time]	88.577 [85.804, 90.681]	85.714 [83.097, 90.007]	85.950 [82.304, 90.086]
$70 \leq G_m \leq 180$ [%time]	99.792 [99.520, 100.000]	99.626 [98.622, 99.911]	98.506 [95.465, 99.787]*
$G_m > 180$ [%time]	0.208 [0.000, 0.481]	0.374 [0.089, 1.378]	1.495 [0.213, 4.536]*
$G_m > 250$ [%time]	0.000 [0.000, 0.000]	0.000 [0.000, 0.000]	0.000 [0.000, 0.000]
$G_m < 70$ [%time]	0.000 [0.000, 0.000]	0.000 [0.000, 0.000]	0.000 [0.000 0.000]
	0.000 (0.000)	0.000 (0.000)	0.128 (0.334)
$G_m < 54$ [%time]	0.000 [0.000, 0.000]	0.000 [0.000, 0.000]	0.000 [0.000, 0.000]
	0.000 (0.000)	0.000 (0.000)	0.000 (0.000)
No. $L1_{hypo}$	0.000 [0.000, 0.000]	0.000 [0.000, 0.000]	0.000 [0.000, 0.000]
	0.000 (0.000)	0.000 (0.000)	0.104 (0.235)
No. $L2_{hypo}$	0.000 [0.000, 0.000]	0.000 [0.000, 0.000]	0.000 [0.000, 0.000]
	0.000 (0.000)	0.000 (0.000)	0.000 (0.000)
TDI [U]	43.754 [40.495, 55.496]	43.576 [40.226, 55.248]	45.233 [41.329, 56.291]
GMI [%]	6.037 [5.994, 6.123]	6.053 [5.999, 6.143]	6.038 [5.952, 6.116]

Table 4
Performance metrics of fully closed-loop scheme (UA_{FCL}) respect to hybrid closed-loop scheme considering announced with 30% error ($A_{30\%}$) and missed announced (UA_{HCL}) cases. An asterisk indicates statistical significance ($p < 0.05$) respect to UA_{FCL} case. (Overall).

	UA_{FCL}	$A_{30\%}$	UA_{HCL}
Mean G_m [mg/dL]	115.955 [113.522, 119.862]	114.673 [112.430, 118.417]	129.222 [122.452, 134.177]*
SD [mg/dL]	27.839 [24.820, 31.446]	21.014 [16.828, 23.827]*	40.037 [29.621, 44.893]*
CV [%]	23.863 [22.532, 26.237]	18.325 [15.030, 19.924]*	29.888 [25.500, 34.188]*
$70 \leq G_m \leq 140$ [%time]	80.653 [79.513, 86.116]	85.714 [83.097, 90.007]	70.722 [68.851, 77.322]*
$70 \leq G_m \leq 180$ [%time]	96.243 [92.570, 97.928]	99.626 [98.622, 99.911]*	84.574 [79.994, 92.347]*
$G_m > 180$ [%time]	3.757 [2.072, 7.430]	0.374 [0.089, 1.378]*	15.426 [7.653, 19.996]*
$G_m > 250$ [%time]	0.000 [0.000, 0.000]	0.000 [0.000, 0.000]	0.188 [0.000, 1.110]*
$G_m < 70$ [%time]	0.000 [0.000, 0.000]	0.000 [0.000, 0.000]	0.000 [0.000, 0.000]
	0.024 (0.056)	0.000 (0.000)	0.0188 (0.0596)
$G_m < 54$ [%time]	0.000 [0.000, 0.000]	0.000 [0.000, 0.000]	0.000 [0.000, 0.000]
	0.000 (0.000)	0.000 (0.000)	0.000 (0.000)
No. $L1_{hypo}$	0.000 [0.000, 0.000]	0.000 [0.000, 0.000]	0.000 [0.000, 0.000]
	0.007 (0.022)	0.000 (0.000)	0.0071 (0.0226)
No. $L2_{hypo}$	0.000 [0.000, 0.000]	0.000 [0.000, 0.000]	0.000 [0.000, 0.000]
	0.000 (0.000)	0.000 (0.000)	0.000 (0.000)
TDI [U]	46.843 [39.082, 53.116]	43.576 [40.226, 55.248]	43.708 [36.709, 48.258]
GMI [%]	6.084 [6.025, 6.177]	6.053 [5.999, 6.143]	6.401 [6.239, 6.519]*

event (i.e., $U_b = u^0(2)$, when the pZMPC is inactive). Table 5 shows that the FIT_{ET} increases the time in tight target by a 15.4% (FIT_{ET} : 82.785% vs FIT_{CT} : 71.746%, $p < 0.05$) without statistical

significant L1 events (no L2 events are reported). Therefore, since the mean glucose is reduced by a 9.15% (FIT_{ET} : 116.334 mg/dL vs FIT_{CT} : 128.0461 mg/dL, $p < 0.05$) and the time in hypoglycemia
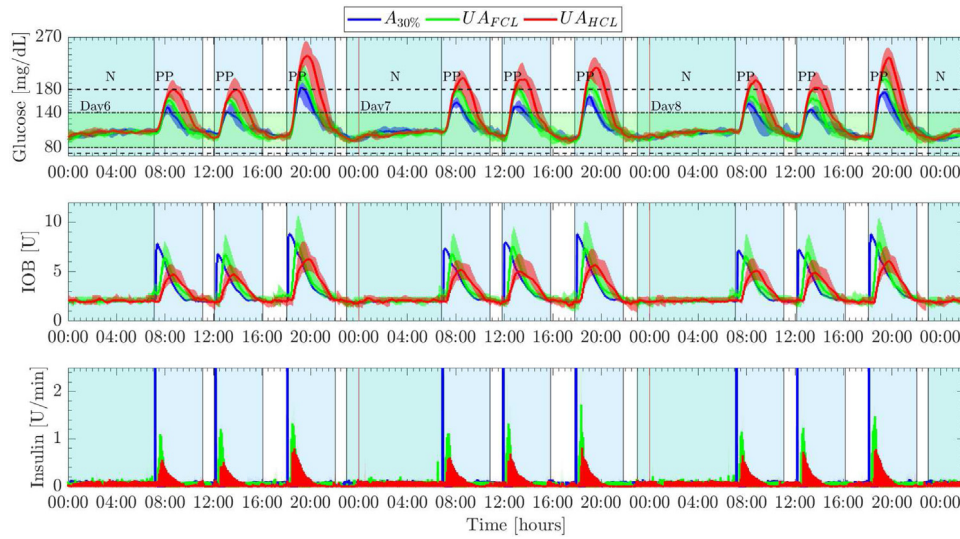
Fig. 7. Comparison of the fully closed-loop scheme (UA_{FCL}) respect to hybrid closed-loop proposal when meals are announced with 30% error($A_{30\%}$) and missed announced (UA_{HCL}). Blood glucose, IOB and insulin profiles are shown in terms of median (solid lines) surrounded by colored regions representing the [25th, 75th] percentiles.
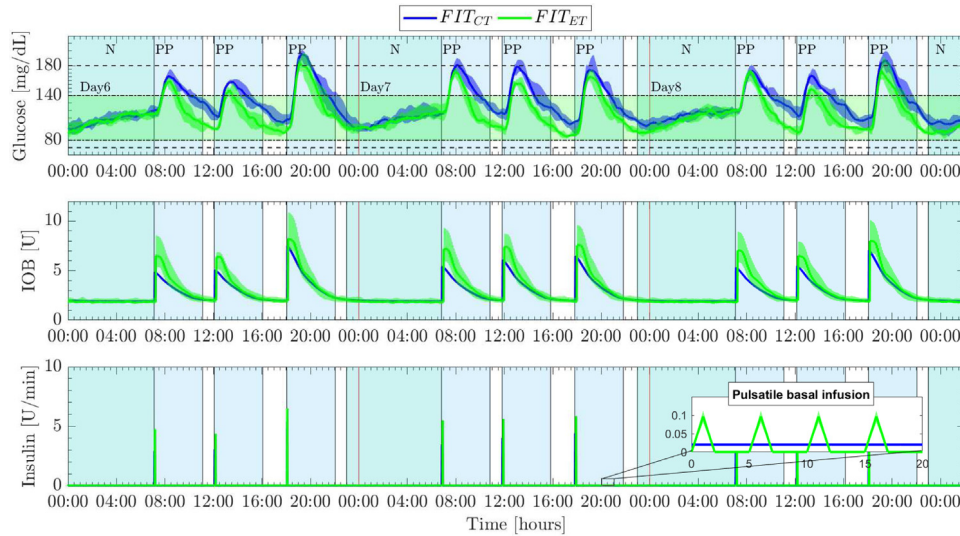
Fig. 8. Comparison of the event-triggered scheme (FIT_{ET}) respect to conventional therapy (FIT_{CT}) under perfectly announced meal case. Blood glucose, IOB and insulin profiles are shown in terms of median (solid lines) surrounded by colored regions representing the [25th, 75th] percentiles.

Table 5
Performance metrics of event-triggered scheme (FIT_{ET}) respect to conventional therapy (FIT_{CT}) set by simulator. An asterisk indicates statistical significance ($p < 0.05$) respect to FIT_{ET} case. (Overall).

	FIT_{ET}	FIT_{CT}
Mean G_m [mg/dL]	116.334 [114.692, 118.451]	128.046 [125.987, 136.855]*
SD [mg/dL]	23.356 [21.490, 28.653]	25.288 [21.574, 28.935]
CV [%]	19.406 [18.651, 24.983]	18.752 [17.917, 22.966]
$70 \leq G_m \leq 140$ [%time]	82.785 [86.547, 86.547]	71.746 [74.864, 74.864]*
$70 \leq G_m \leq 180$ [%time]	98.999 [99.371, 99.371]	96.572 [95.930, 95.930]
$G_m > 180$ [%time]	1.001 [0.630, 0.630]	3.428 [4.070, 4.070]
$G_m > 250$ [%time]	0.000 [0.000, 0.000]	0.000 [0.000, 0.000]
$G_m < 70$ [%time]	0.000 [0.000, 0.000]	0.000 [0.000, 0.000]
	0.0169 (0.0533)	0.000 (0.000)
$G_m < 54$ [%time]	0.000 [0.000, 0.000]	0.000 [0.000, 0.000]
	0.000 (0.000)	0.000 (0.000)
No. $L1_{hypo}$	0.000 [0.000, 0.000]	0.000 [0.000, 0.000]
	0.0071 (0.0226)	0.000 (0.000)
No. $L2_{hypo}$	0.000 [0.000, 0.000]	0.000 [0.000, 0.000]
	0.000 (0.000)	0.000 (0.000)
TDI [U]	46.551 [39.497, 52.454]	43.111 [37.051, 47.080]
GMI [%]	6.093 [6.053, 6.143]	6.373 [6.324, 6.584]*

range is not significant, the proposed strategy would impact on a enhancement of A1c management (GMI, FIT_{ET} : 6.093% vs FIT_{CT} : 6.373%, $p = 0.005$). In this context, the proposed controller could be used as an optimal basal–bolus calculator, designed for computing both, basal and bolus infusions, according to the solution of an optimization problem.

8. Conclusion

An AP based on a stable pZMPC with individualized model was proposed. The approach aims to steer blood glucose to target zone, by employing a pulsatile insulin administration for both, basal and bolus infusions. A daily state set considering normoglycemia range as well as insulin on board constraints was included in order to restrict the insulin infusion, especially during post prandial periods (i.e.: due to overestimated meal intake) and night intervals (i.e.: due to insulin stacking, circadian variability of insulin sensitivity, missing out a dinner, etc.). Furthermore, the presented controller was implemented taking into account announced as well as unannounced meal intake, employing dedicated disturbance observers. For the announced case (hybrid closed-loop scheme) the controller administrates insulin in a super-bolus mode since a fully carbohydrate meal ingest rate (during a sampling period) is assumed. Moreover, the performance was not significantly degraded when meals were announced with 30% error ($A_{30\%}$). On the other hand, for the unannounced case (fully closed-loop scheme, U_{FCL}), the Ra estimation (by means of an input disturbance observer) allowed an improvement of glycemia control respect to missed announced case (U_{HCL}). Moreover, this formulation achieved a behavior comparable with the hybrid scheme under regular carb counting misestimation errors ($A_{30\%}$). Furthermore, the $A_{30\%}$ and U_{FCL} cases were assessed considering circadian variability of insulin sensitivity, with not significant differences respect to nominal case. To take advantage of the pulsatile mode, the proposed controller was finally used as an optimal basal–bolus calculator. A better glycemia control respect to conventional FIT therapy was obtained thanks to the explicit use of predictions, state and inputs constraints, and asymmetric stage costs. Future research includes the explicit use of time-variant linear/nonlinear model for predictions, to better account for any kind a variability.

Appendx

Next, the detailed steps to obtain discrete-time system (9) from the sampling of the continuous-time one (4), considering the pulsatile input (8) and constant meals along the period are given. The continuous-time solution of (4), on each periods T, can be written as:
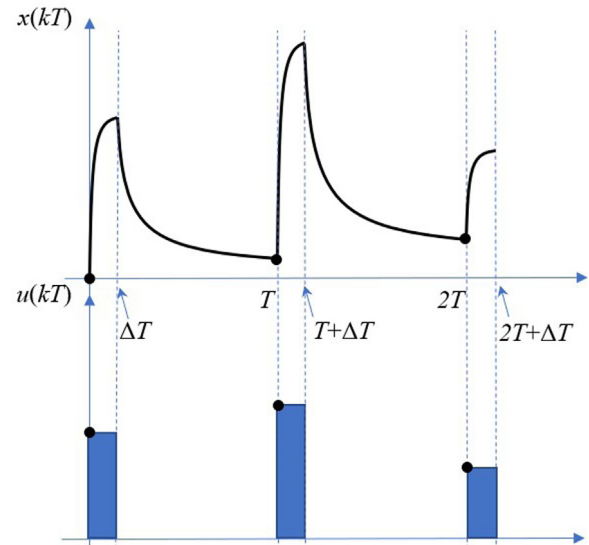
$$x(t) = \varphi(t; x(kT), u(\cdot), r(\cdot))$$

Fig. 9. Pulsive scheme. Continuous-time evolution and sampled system.

$$= e^{A(t-kT)}x(kT) + \int_{kT}^{t} e^{A(t-\zeta)}B_u u(\zeta)d\zeta$$
$$+ \int_{kT}^{t} e^{A(t-\zeta)}d\zeta B_r r(kT) + \int_{kT}^{t} e^{A(t-\zeta)}d\zeta E,$$

for $t \in [kT, (k + 1)T]$, where the disturbance r is now out of the integral, because it is constant all along the time period $[kT, (k+1)T)$. To obtain a discrete-time system, the latter solution is sampled at times $t = kT, k \in \mathbb{N}$. Furthermore, taking into account that input $u(t)$ is null in $[kT + \Delta T, (k + 1)T)$, it follows that:

$$x((k + 1)T) = e^{A((k+1)T-kT)}x(kT) + \int_{kT}^{kT+\Delta T} e^{A((k+1)T-\zeta)}d\zeta B_u u(kT)$$
$$+ \int_{kT}^{(k+1)T} e^{A((k+1)T-\zeta)}d\zeta B_r r(kT)$$
$$+ \int_{kT}^{(k+1)T} e^{A((k+1)T-\zeta)}d\zeta E.$$

Given that the model matrices are time-invariant, we can consider $kT = 0$ in the integrals, without loss of generality, and so

$$x((k + 1)T) = e^{AT}x(kT) + \int_{0}^{\Delta T} e^{A(T-\zeta)}d\zeta B_u u(kT) \qquad (12)$$
$$+ \int_{0}^{T} e^{A(T-\zeta)}d\zeta B_r r(kT) + \int_{0}^{T} e^{A(T-\zeta)}d\zeta E.$$

But the second term of the latter equation can be written as

$$\int_{0}^{\Delta T} e^{A(T-\zeta)}d\zeta B_u u(kT) = e^{A(T-\Delta T)} \int_{0}^{\Delta T} e^{A(\Delta T-\zeta)}d\zeta B_u u(kT)$$

and then, Eq. (12) reads

$$x((k + 1)T) = e^{AT}x(kT) + e^{A(T-\Delta T)} \int_{0}^{\Delta T} e^{A(\Delta T-\zeta)}d\zeta B_u u(kT)$$
$$+ \int_{0}^{T} e^{A(T-\zeta)}d\zeta B_r r(kT)$$
$$+ \int_{0}^{T} e^{A(T-\zeta)}d\zeta E$$
$$= A^d x(kT) + B_u^d u(kT) + B_r^d r(kT) + E^d$$

where $A^d = e^{AT}$, $B_u^d = e^{A(T-\Delta T)} \int_0^{\Delta T} e^{A(\Delta T - \zeta)} d\zeta B_u = e^{A(T-\Delta T)} A^{-1}(e^{A\Delta T} - I_5)B_u$, $B_r^d = \int_0^T e^{A(T-\zeta)} d\zeta B_r = A^{-1}(e^{AT} - I_5)B_r$ and $E^d = \int_0^T e^{A(T-\zeta)} d\zeta E = A^{-1}(e^{AT} - I_5)E$. Fig. 9 shows an schematic plot of the pulsatile evolution of a system, where it can be seen that there are two different components: the first one corresponds to the response forced by the input u, while the other is a free response.

References

[1] I.D. Atlas, S. Edition, Online version of IDF diabetes atlas, 2015, Available at: www.diabetesatlas.org.

[2] A. Katsarou, S. Gudbjörnsdottir, A. Rawshani, D. Dabelea, E. Bonifacio, B.J. Anderson, L.M. Jacobsen, D.A. Schatz, Å. Lernmark, Type 1 diabetes mellitus, Nat. Rev. Dis. Primers 3 (2017) 17016.

[3] American Diabetes Association, Classification and diagnosis of diabetes: standards of medical care in diabetes—2019, Diabetes Care 42 (Supplement 1) (2019) S13–S28.

[4] American Diabetes Association, Glycemic targets: Standards of medical care in diabetes-2019, Diabetes Care 42 (Supplement 1) (2019) S61–S70.

[5] J. Walsh, R. Roberts, Pumping Insulin: Everything for Success on an Insulin Pump and CGM, Torrey Pines Press, 2017.

[6] K. Howorka, Functional Insulin Treatment: Principles, Teaching Approach and Practice, Springer Science & Business Media, 2012.

[7] C. Cobelli, E. Renard, B. Kovatchev, Artificial pancreas: past, present, future, Diabetes 60 (11) (2011) 2672–2682.

[8] S. Trevitt, S. Simpson, A. Wood, Artificial pancreas device systems for the closed-loop control of type 1 diabetes: what systems are in development? J. Diabetes Sci. Technol. 10 (3) (2016) 714–723.

[9] G.M. Steil, Algorithms for a closed-loop artificial pancreas: the case for proportional-integral-derivative control, J. Diabetes Sci. Technol. 7 (6) (2013) 1621–1631.

[10] R. Mauseth, I.B. Hirsch, J. Bollyky, R. Kircher, D. Matheson, S. Sanda, C. Greenbaum, Use of a "fuzzy logic" controller in a closed-loop artificial pancreas, Diabetes Technol. Ther. 15 (8) (2013) 628–633.

[11] M. Messori, G.P. Incremona, C. Cobelli, L. Magni, Individualized model predictive control for the artificial pancreas: In silico evaluation of closed-loop glucose control, IEEE Control Syst. Mag. 38 (1) (2018) 86–104.

[12] A. Haidar, The artificial pancreas: How closed-loop control is revolutionizing diabetes, IEEE Control Syst. Mag. 36 (5) (2016) 28–47.

[13] D. Shi, S. Deshpande, E. Dassau, F.J. Doyle III, Feedback control algorithms for automated glucose management in T1DM: the state of the art, in: The Artificial Pancreas, Elsevier, 2019, pp. 1–27.

[14] G.P. Incremona, M. Messori, C. Toffanin, C. Cobelli, L. Magni, Model predictive control with integral action for artificial pancreas, Control Eng. Pract. 77 (2018) 86–94.

[15] R. Hovorka, et al., Nonlinear model predictive control of glucose concentration in subjects with type-1 diabetes, Physiol. Meas. 25 (4) (2004) 905–920.

[16] R. Gondhalekar, E. Dassau, F.J. Doyle III, Velocity-weighting and velocity-penalty MPC of an artificial pancreas: Improved safety and performance, Automatica 91 (48) (2018) 105–117.

[17] D. Boiroux, A.K. Duun-Henriksen, S. Schmidt, K. Nørgaard, S. Madsbad, N.K. Poulsen, H. Madsen, J.B. Jørgensen, Overnight glucose control in people with type 1 diabetes, Biomed. Signal Process. Control 39 (2018) 503–512.

[18] I. Hajizadeh, M. Rashid, S. Samadi, M. Sevil, N. Hobbs, R. Brandt, A. Cinar, Adaptive personalized multivariable artificial pancreas using plasma insulin estimates, J. Process Control 80 (2019) 26–40.

[19] D. Shi, E. Dassau, F.J. Doyle III, Multivariate learning framework for long-term adaptation in the artificial pancreas, Bioeng. Transl. Med. 4 (1) (2019) 61–74.

[20] D. Boiroux, V. Bátora, M. Hagdrup, S.L. Wendt, N.K. Poulsen, H. Madsen, J.B. Jørgensen, Adaptive model predictive control for a dual-hormone artificial pancreas, J. Process Control 68 (2018) 105–117.

[21] G.C. Goodwin, A.M. Medioli, H.V. Phan, B.R. King, A.D. Matthews, Application of MPC incorporating stochastic programming to type 1 diabetes treatment, in: 2016 American Control Conference, ACC, IEEE, 2016, pp. 907–912.

[22] M.M. Seron, A.M. Medioli, G.C. Goodwin, A methodology for the comparison of traditional MPC and stochastic MPC in the context of the regulation of blood glucose levels in type 1 diabetics, in: 2016 Australian Control Conference, AuCC, IEEE, 2016, pp. 126–131.

[23] C.D. Man, F. Micheletto, D. Lv, M. Breton, B. Kovatchev, C. Cobelli, The UVA/Padova type 1 diabetes simulator: new features, J. Diabetes Sci. Technol. 8 (1) (2014) 26–34.

[24] R. Hovorka, F. Shojaee-Moradie, P.V. Carroll, L.J. Chassin, I.J. Gowrie, N.C. Jackson, R.S. Tudor, A.M. Umpleby, R.H. Jones, Partitioning glucose distribution/transport, disposal, and endogenous production during IVGTT, Am. J. Physiol. Endocrinol. Metab. 282 (5) (2002) E992–E1007.

[25] S.S. Kanderian, S. Weinzimer, G. Voskanyan, G.M. Steil, Identification of Intraday Metabolic Profiles During Closed-Loop Glucose Control in Individuals with Type 1 Diabetes, SAGE Publications, 2009.

[26] J.B. Jørgensen, D. Boiroux, Z. Mahmoudi, An artificial pancreas based on simple control algorithms and physiological insight, IFAC-PapersOnLine 52 (1) (2019) 1018–1023.

[27] DiabetesHealth, Product reference guide january 2019, 2019, Available at: https://diabeteshealth.com/wp-content/uploads/2019/pdf/2019/InsulinPumps.pdf.

[28] S.H. Song, S.S. McIntyre, H. Shah, J.D. Veldhuis, P.C. Hayes, P.C. Butler, Direct measurement of pulsatile insulin secretion from the portal vein in human subjects, J. Clin. Endocrinol. Metab. 85 (12) (2000) 4491–4499.

[29] L.S. Satin, P.C. Butler, J. Ha, A.S. Sherman, Pulsatile insulin secretion, impaired glucose tolerance and type 2 diabetes, Mol. Aspects. Med. 42 (2015) 61–77.

[30] W. Regittnig, M. Urschitz, B. Lehki, M. Wolf, H. Kojzar, J.K. Mader, M. Ellmerer, T.R. Pieber, Insulin bolus administration in insulin pump therapy: Effect of bolus delivery speed on insulin absorption from subcutaneous tissue, Diabetes Technol. Ther. 21 (1) (2019) 44–50.

[31] G.C. Goodwin, A.M. Medioli, D.S. Carrasco, B.R. King, Y. Fu, A fundamental control limitation for linear positive systems with application to type 1 diabetes treatment, Automatica 55 (2015) 73–77.

[32] G.C. Goodwin, D.S. Carrasco, M.M. Seron, A.M. Medioli, A fundamental control performance limit for a class of positive nonlinear systems, Automatica 95 (2018) 14–22.

[33] H.M. Tolic, E. Mosekilde, J. Stuirs, Modeling the insulin-glucose feedback system: the significance of pulsatile insulin secretion, J. Theoret. Biol. 207 (2000) 361–375.

[34] Y. Ruan, M.E. Wilinska, H. Thabit, R. Hovorka, Modeling day-to-day variability of glucose-insulin regulation over 12-week home use of closed-loop insulin delivery, IEEE Trans. Biomed. Eng. 64 (6) (2017) 1412–1419.

[35] P.S. Rivadeneira, A. Ferramosca, A.H. González, Control strategies for non-zero set-point regulation of linear impulsive systems, IEEE Trans. Automat. Control 69 (9) (2018) 2994–3001.

[36] P.S. Rivadeneira, J.L. Godoy, J.E. Serenoa, P. Abuin, A. Ferramosca, A.H. González, Impulsive MPC schemes for biomedical processes. Application to type 1 diabetes, in: A.T. Azar (Ed.), Control Applications for Biomedical Engineering Systems, ELSEVIER, 2019.

[37] C.M. Ramkisson, P. Herrero, J. Bondia, V. J., Unannounced meals in the artificial pancreas: Detection using continuous glucose monitoring, Sensors 18 (2018) 1–18, http://dx.doi.org/10.3390/s18030884.

[38] A. El Fathi, M.R. Smaoui, V. Gingras, B. Boulet, A. Haidar, The artificial pancreas and meal control: an overview of postprandial glucose regulation in type 1 diabetes, IEEE Control Syst. Mag. 38 (1) (2018) 67–85.

[39] S. Oviedo, J. Vehí, R. Calm, J. Armengol, A review of personalized blood glucose prediction strategies for T1DM patients, Int. J. Numer. Methods Biomed. Eng. 33 (6) (2017) e2833.

[40] E.M. Aiello, G. Lisanti, L. Magni, M. Musci, C. Toffanin, Therapy-driven deep glucose forecasting, Eng. Appl. Artif. Intell. 87 (2020) 103255.

[41] C.D. Man, R.A. Rizza, C. Cobelli, Meal simulation model of the glucose-insulin system, IEEE Trans. Biomed. Eng. 54 (10) (2007) 1740–1749.

[42] R.N. Bergman, Y.Z. Ider, C.R. Bowden, C. Cobelli, Quantitative estimation of insulin sensitivity, Am. J. Physiol. Endocrinol. Metab. 236 (6) (1979) E667.

[43] I. Hajizadeh, M. Rashid, K. Turksoy, S. Samadi, J. Feng, M. Sevil, N. Frantz, C. Lazaro, Z. Maloney, E. Littlejohn, et al., Multivariable recursive subspace identification with application to artificial pancreas systems, IFAC-PapersOnLine 50 (1) (2017) 886–891.

[44] K. van Heusden, E. Dassau, H.C. Zisser, D.E. Seborg, F.J. Doyle III, Control-relevant models for glucose control using a priori patient characteristics, IEEE Trans. Biomed. Eng. 59 (7) (2011) 1839–1849.

[45] M. Messori, C. Toffanin, S. Del Favero, G. De Nicolao, C. Cobelli, L. Magni, Model individualization for artificial pancreas, Comput. Methods Programs Biomed. (2016).

[46] C. Cobelli, G. Pacini, G. Toffolo, L. Sacca, Estimation of insulin sensitivity and glucose clearance from minimal model: new insights from labeled IVGTT, Am. J. Physiol. Endocrinol. Metab. 250 (5) (1986) E591–E598.

[47] N. Magdelaine, L. Chaillous, I. Guilhem, J.Y. Poirier, M. Krempf, C.H. Moog, E.L. Carpentier, A long-term model of the glucose-insulin dynamics of type 1 diabetes, IEEE Trans. Biomed. Eng. 62 (6) (2015) 1546–1552.

[48] S. Dube, I. Errazuriz-Cruzat, A. Basu, R. Basu, The forgotten role of glucose effectiveness in the regulation of glucose tolerance, Curr. Diabetes Rep. 15 (6) (2015) 31.

[49] J. Bondia, S. Romero-Vivo, B. Ricarte, J.L. Diez, Insulin estimation and prediction: a review of the estimation and prediction of subcutaneous insulin pharmacokinetics in closed-loop glucose control, IEEE Control Syst. Mag. 38 (1) (2018) 47–66.

[50] P. Colmegna, F. Garelli, H. De Battista, R. Sánchez-Peña, Automatic regulatory control in type 1 diabetes without carbohydrate counting, Control Eng. Pract. 74 (2018) 22–32.

[51] C. Cobelli, E. Carson, Introduction to Modeling in Physiology and Medicine, Academic Press, 2019.

[52] D. Simon, Kalman filtering with state constraints: a survey of linear and nonlinear algorithms, IET Control Theory Appl. 4 (8) (2010) 1303–1318.

[53] P. Rivadeneira, A. Ferramosca, A.H. González, MPC with state window target control in linear impulsive systems, IFAC-PapersOnline 48 (23) (2015) 507–512.

[54] T. Alamo, A. Ferramosca, A.H. González, D. Limon, D. Odloak, A gradient-based strategy for the one-layer RTO+MPC controller, J. Process Control 24 (4) (2014) 435–447.

[55] A. Ferramosca, A.H. González, D. Limon, Offset-free multi-model economic model predictive control for changing economic criterion, J. Process Control 54 (2017) 1–13.

[56] M. Vettoretti, A. Facchinetti, G. Sparacino, C. Cobelli, Type-1 diabetes patient decision simulator for in silico testing safety and effectiveness of insulin treatments, IEEE Trans. Biomed. Eng. 65 (6) (2017) 1281–1290.

[57] T. Danne, R. Nimri, T. Battelino, R.M. Bergenstal, K.L. Close, J.H. DeVries, S. Garg, L. Heinemann, I. Hirsch, S.A. Amiel, et al., International consensus on use of continuous glucose monitoring, Diabetes Care 40 (12) (2017) 1631–1640.

[58] R.M. Bergenstal, R.W. Beck, K.L. Close, G. Grunberger, D.B. Sacks, A. Kowalski, A.S. Brown, L. Heinemann, G. Aleppo, D.B. Ryan, et al., Glucose management indicator (GMI): a new term for estimating A1C from continuous glucose monitoring, Diabetes Care 41 (11) (2018) 2275–2280.

[59] T. Kawamura, C. Takamura, M. Hirose, T. Hashimoto, T. Higashide, Y. Kashihara, K. Hashimura, H. Shintaku, The factors affecting on estimation of carbohydrate content of meals in carbohydrate counting, Clin. Pediatric Endocrinol. 24 (4) (2015) 153–165.

[60] E.J. Mansell, P.D. Docherty, J.G. Chase, Shedding light on grey noise in diabetes modelling, Biomed. Signal Process. Control 31 (2017) 16–30.